

Table 2
Frequency of genotypes VAV2 and VAV3 gene in patients with POAG, NTG and in controls in Japanese.

	POAG (n = 168)	NTG (n = 163)	DG (n = 45)	Control (n = 180)
VAV2 (rs2156323 A/G)				
G/G	151 (89.9%)	147 (90.2%)	43 (95.6%)	168 (93.3%)
G/A	17 (10.1%)	16 (9.8%)	2 (4.4%)	11 (6.1%)
A/A	0 (0%)	0 (0%)	0 (0%)	1 (0.6%)
P value*	0.25	0.29	0.80	
VAV3 (rs2801219 A/C)				
A/A	108 (64.3%)	92 (56.4%)	25 (55.6%)	119 (66.1%)
A/C	49 (29.2%)	65 (39.9%)	18 (40.0%)	51 (28.3%)
C/C	11 (6.5%)	6 (3.7%)	2 (4.4%)	10 (5.6%)
P value*	0.90	0.07	0.32	

Data presented are number of patients, unless otherwise indicated. The asterisk indicates that the significance of the association was determined by a contingency table analysis using the χ^2 test.

($P = 0.32$) groups than in the control group (Table 2). The SNP adhered to the Hardy–Weinberg expectations ($P > 0.05$).

3.3. Dominant and recessive model for rs2156323 SNP in VAV2 and rs2801219 SNP in VAV3

The homozygotes for the rs2156323 SNP A/A were 0% in the glaucoma subjects, and 0.6% in the control subjects ($P > 0.05$; Table 2). We analyzed the dominant and recessive model for the rs2801219 SNP in VAV3 (Table 3). There was also no significant difference between the subgroups of glaucoma and SNP rs2801219 in VAV3. However, in the NTG group, P was 0.06 for the dominant model.

4. Discussion

Obtaining evidence that candidate genes and gene variants are significantly associated with a specific disease is more biologically meaningful when the same associations are also found in different ethnic populations. The significant associations would then indicate that these genes play a role in the pathogenesis of the disease [13]. Our findings showed that the alleles rs2156323 (VAV2) and rs2801219 (VAV3) were not significantly associated with POAG in Japanese patients. These risk alleles were also not significantly associated with POAG or primary angle closure glaucoma (PACG) in Indian cohorts [13]. It has also been reported that the genotype frequencies at these loci were not significantly different among POAG, PACG, and control subjects in Indian cohorts [14].

The finding that *Vav2*-deficiency alone resulted in a glaucoma phenotype in mice suggested that the absence of *Vav2* is associated with the development of glaucoma in mice. However, our findings demonstrated that there was no significant association between the VAV2 SNP and POAG, NTG, and DG. In addition, the VAV2 SNP rs2156323 was not associated with these glaucoma phenotypes. Functionally, the *Vav2/Vav3*-deficient (*Vav2*^{-/-}/*Vav3*^{-/-}) mice had buphthalmos and iridocorneal changes that altered the aqueous outflow that lead to elevated intraocular pressure. The optic nerve head cupping resembled that found in developmental glaucoma

and PACG. Thus, we hypothesized that VAV2 and VAV3 could be major candidate genes for developmental glaucoma in humans. However, our results showed that DG, POAG and NTG were not significantly associated with alleles rs2156323 (VAV2) and rs2801219 (VAV3) (Tables 1 and 2). We also compared the DG group with an age-matched young control group ($n = 60$; 30.4 ± 6.2 years). Neither the frequencies of the A allele of VAV2 rs2156323 (DG 0.022 and young controls 0.075; $P = 0.09$, chi-square test), nor the C allele of rs2801219 (DG 0.244 and young controls 0.175; $P = 0.22$, chi-square test) was significantly different from young controls (data not shown).

There is a possibility that the lack of significant associations at these loci in our POAG cases could have been due to clinical heterogeneity.

Another possibility for the lack of significant associations is the sample size because small sample sizes are known to cause a type II error. There were 45 DG cases and 180 controls for a total of 225 subjects. For an effect size = 0.3 (medium), an α error probability of 0.05, and a degree of freedom (Df) = 2, the power (1 – beta error probability) is 98.6%. However, for an effect size = 0.1 (small), an α error probability of 0.05, and a Df = 2, the power is only 24.9%. To obtain a power of 80% under the same conditions, the total sample size must be 964 cases.

The Vav family of proteins consists of a group of signal transduction molecules with oncogenic potential that play important roles in development and cell signaling. The best known function of the Vav proteins is their role as GDP/GTP exchange factors that activate Rho guanosine triphosphatases (GTPases) in a phosphorylation-dependent manner [15]. In addition to their function as exchange factors, the evidence increasingly suggests that Vav proteins can mediate other cellular functions, most likely as adaptor molecules. Deregulation of the GDP/GTP exchange is one possible mechanism for the alterations that lead to iridocorneal angle closure. Thus, we suggest that VAV2 and VAV3 may still be candidate genes for PACG, and the association between Vav2/Vav3 and PACG deserves further study.

In summary, the variants rs2156323 in the VAV2 gene and rs2801219 in the VAV3 gene do not appear to be major risk factors for the pathogenesis of glaucoma in the Japanese. However, Vav2/

Table 3
Frequency of genotypes in dominant or recessive model in VAV3 gene in patients with POAG, NTG and in controls in Japanese.

VAV3 (rs2801219 A/C)		POAG (n = 168)	NTG (n = 163)	DG (n = 45)	Control (n = 180)
Dominant	A/A	108 (64.3%)	92 (56.4%)	25 (55.6%)	119 (66.1%)
	A/C + C/C	60 (35.7%)	71 (43.6%)	20 (44.4%)	61 (33.9%)
P value*		0.72	0.06	0.19	
Recessive	A/A + A/C	157 (93.5%)	157 (96.3%)	43 (95.6%)	170 (94.4%)
	C/C	11 (6.5%)	6 (3.7%)	2 (4.4%)	10 (5.6%)
P value*		0.70	0.41	0.77	

Data presented are number of patients, unless otherwise indicated. The asterisk indicates that the significance of the association was determined by a contingency table analysis using the χ^2 test.

Vav3-deficient mice can still serve as useful models for the study of spontaneous glaucoma, and investigations into the development of the phenotype may provide information on the pathogenesis of glaucoma in humans.

Disclosure

D. Shi, None; Y. Takano, None; M.T. Nakazawa, None; Mengke-gale, None; S. Yokokura; None, K. Nishida, None; N. Fuse, None.

Acknowledgments

The authors thank Dr. Duco I. Hamasaki for editing the manuscript. This study was supported in part by a Grant-In-Aid for Scientific Research from the Ministry of Education, Science, and Culture of the Japanese Government (NF; C-22591928), by grant from the Ministry of Health, Labor, and Welfare of Japan to N.F., and by a grant from the Japan–China Medical Association to D.S.

References

- [1] H.A. Quigley, Number of people with glaucoma worldwide, *Br. J. Ophthalmol.* 80 (1996) 389–393.
- [2] D. Gupta, *Glaucoma diagnosis and management*, Lippincott Williams & Wilkins, Philadelphia, 2005.
- [3] Y. Shiose, Y. Kitazawa, S. Tsukahara, T. Akamatsu, K. Mizokami, R. Futa, H. Katsushima, H. Kosaki, Epidemiology of glaucoma in Japan – a nationwide glaucoma survey, *Jpn. J. Ophthalmol.* 35 (1991) 133–155.
- [4] A. Iwase, Y. Suzuki, M. Araie, T. Yamamoto, H. Abe, S. Shirato, Y. Kuwayama, H.K. Mishima, H. Shimizu, G. Tomita, Y. Inoue, Y. Kitazawa, The prevalence of primary open-angle glaucoma in Japanese: the Tajimi Study, *Ophthalmology* 111 (2004) 1641–1648.
- [5] V. Raymond, Molecular genetics of the glaucomas: mapping of the first five “GLC” loci, *Am. J. Hum. Genet.* 60 (1997) 272–277.
- [6] M. Sarfarazi, Recent advances in molecular genetics of glaucomas, *Hum. Mol. Genet.* 6 (1997) 1667–1677.
- [7] E.M. Stone, J.H. Fingert, W.L. Alward, T.D. Nguyen, J.R. Polansky, S.L. Sundén, D. Nishimura, A.F. Clark, A. Nystuen, B.E. Nichols, D.A. Mackey, R. Ritch, J.W. Kalenak, E.R. Craven, V.C. Sheffield, Identification of a gene that causes primary open angle glaucoma, *Science* 275 (1997) 668–670.
- [8] T. Rezaie, A. Child, R. Hitchings, G. Brice, L. Miller, M. Coca-Prados, E. Heon, T. Krupin, R. Ritch, D. Kreutzer, R.P. Crick, M. Sarfarazi, Adult-onset primary open-angle glaucoma caused by mutations in optineurin, *Science* 295 (2002) 1077–1079.
- [9] S. Monemi, G. Spaeth, A. DaSilva, S. Popinchalk, E. Ilitchev, J. Liebmann, R. Ritch, E. Heon, R.P. Crick, A. Child, M. Sarfarazi, Identification of a novel adult-onset primary open-angle glaucoma (POAG) gene on 5q22.1, *Hum. Mol. Genet.* 14 (2005) 725–733.
- [10] K. Fujikawa, T. Iwata, K. Inoue, M. Akahori, H. Kadotani, M. Fukaya, M. Watanabe, Q. Chang, E.M. Barnett, W. Swat, VAV2 and VAV3 as candidate disease genes for spontaneous glaucoma in mice and humans, *PLoS One* 5 (2010) e9050.
- [11] J.H. Zhao, D. Curtis, P.C. Sham, Model-free analysis and permutation tests for allelic associations, *Hum. Hered.* 50 (2000) 133–139.
- [12] F. Faul, E. Erdfelder, A.G. Lang, A. Buchner, G*Power 3: a flexible statistical power analysis program for the social, behavioral, and biomedical sciences, *Behav. Res. Methods* 39 (2007) 175–191.
- [13] S.J. Chanock, T. Manolio, M. Boehnke, E. Boerwinkle, D.J. Hunter, G. Thomas, J.N. Hirschhorn, G. Abecasis, D. Altshuler, J.E. Bailey-Wilson, L.D. Brooks, L.R. Cardon, M. Daly, P. Donnelly, J.F. Fraumeni Jr., N.B. Freimer, D.S. Gerhard, C. Gunter, A.E. Guttmacher, M.S. Guyer, E.L. Harris, J. Hoh, R. Hoover, C.A. Kong, K.R. Merikangas, C.C. Morton, L.J. Palmer, E.G. Phimister, J.P. Rice, J. Roberts, C. Rotimi, M.A. Tucker, K.J. Vogan, S. Wacholder, E.M. Wijsman, D.M. Winn, F.S. Collins, Replicating genotype–phenotype associations, *Nature* 447 (2007) 655–660.
- [14] K.N. Rao, I. Kaur, R.S. Parikh, A.K. Mandal, G. Chandrasekhar, R. Thomas, S. Chakrabarti, Variations in NTF4, VAV2, and VAV3 genes are not involved with primary open-angle and primary angle-closure glaucomas in an Indian population, *Invest. Ophthalmol. Vis. Sci.* 51 (2010) 4937–4941.
- [15] X.R. Bustelo, Vav proteins, adaptors and cell signaling, *Oncogene* 20 (2001) 6372–6381.

Development of Genetically Modified Eliminable Human Dermal Fibroblast Feeder Cells for Ocular Surface Regeneration Medicine

Yingli Li,¹ Tomoyuki Inoue,² Fumihiko Takamatsu,¹ Naoyuki Maeda,¹ Yuichi Ohashi,² and Kohji Nishida¹

¹Department of Ophthalmology, Osaka University Medical School, Suita, Japan

²Department of Ophthalmology, Ehime University, Ehime, Japan

Correspondence: Tomoyuki Inoue, Department of Ophthalmology, Ehime University School of Medicine, Shitsukawa, Toon-City, Ehime, 791-0295, Japan; tomonoue@m.ehime-u.ac.jp.

Submitted: July 19, 2013

Accepted: September 23, 2013

Citation: Li Y, Inoue T, Takamatsu F, Maeda N, Ohashi Y, Nishida K. Development of genetically modified eliminable human dermal fibroblast feeder cells for ocular surface regeneration medicine. *Invest Ophthalmol Vis Sci.* 2013;54:7522-7531. DOI:10.1167/iops.13-12870

PURPOSE. Cultured human corneal limbal stem/progenitor cells are usually established and maintained on feeder layers. However, animal feeder cells are associated with viral infection, pathogen transmission, and xenogenic contamination. All feeder cells also can be mixed easily into cell-sheet production, causing self-contamination. We developed a line of labeled, immortalized, eliminable human dermal fibroblast cells to eliminate these problems.

METHODS. The enhanced green fluorescent protein gene, human-derived telomerase reverse transcriptase gene, and herpes simplex virus thymidine kinase gene were transfected into human dermal fibroblast cells to establish labeled, immortalized, eliminable feeder cells. Established eliminable dermal fibroblasts (TERT+TK-D) were treated with mitomycin, cocultured with human limbal stem/progenitor cells to regenerate epithelium sheets, and compared with 3T3 feeder cells.

RESULTS. Established TERT+TK-D feeder cells maintained immortalization, visualization, and eliminable characteristics during 6 months of continuous passages. The colony-forming efficiency of limbal stem/progenitor cells was similar in the TERT+TK-D group ($11.77 \pm 0.21\%$) and the 3T3 group ($12.8 \pm 1.61\%$) ($P = 0.332$). All cell sheets were well stratified into 4 to 5 layers. The TERT+TK-D group colonies and epithelial cell sheets showed weaker staining of corneal epithelium differentiation marker K3 than the 3T3 group and quantitative analysis of mRNA transcripts. Moreover, PCR analysis against the long terminal repeat sequence of the lentiviral vector integrated into the genetically modified feeder cells showed no contamination of ganciclovir-treated regeneration epithelial sheets.

CONCLUSIONS. Genetically modified, labeled, immortalized, eliminable human dermal feeder cells are promising substitutes for 3T3 feeder cells for xenogeny-free ocular surface regeneration.

Keywords: corneal epithelium, eliminable feeder cell, human dermal fibroblast

Both limbal stem/progenitor cells and oral epithelial cells have been used successfully in ocular surface regeneration medicine to treat severe ocular surface disorders.¹⁻⁴ However, the murine 3T3 fibroblast feeder cells used in the technique can transmit murine diseases to patients. Recent reports have indicated that human embryonic stem cell lines cultured on murine feeder cells express the murine xenoantigen Neu5Gc and can induce immune reactions in humans.^{5,6} Therefore, it is necessary to find an effective and safe human-derived feeder cell to substitute for the murine 3T3 cells.

Several recent studies have reported that a promising alternative to murine 3T3 cells might be human dermal fibroblasts used as a feeder layer to coculture with limbal and oral epithelial cells, which have the ability to maintain the growth and stem cell characteristics of corneal and oral epithelium.^{7,8} However, the finite proliferative lifespan of normal human cells cultured in vitro could prevent clinical application of dermal fibroblast feeder cells because of increasing workload and costs. Moreover, all kinds of feeder

cells can mix easily into cell-sheet production, causing self-contamination.

We have previously⁹ developed a new culture technique of eliminable, feeder-assisted target cell-sheet production and reported the efficacy of the genetically modified human-derived feeder cell line with the properties of immortalization, labeling, and elimination. In the current study, our goal was to develop a genetically modified human dermal fibroblast feeder cell line with immortalization, labeling, and elimination characteristics. We compared the characteristics of the epithelial colonies and sheets that were cocultured with genetically modified dermal fibroblast cells and 3T3 fibroblast cells. We found that genetically modified dermal fibroblast cells maintained the ability to support limbal stem/progenitor cell growth and differentiation and prevented feeder cell self-contamination. The genetically modified, labeled, immortalized, eliminable human dermal feeder cell is a promising alternative for 3T3 feeder cells in the clinical application of xenogeny-free ocular surface regeneration.

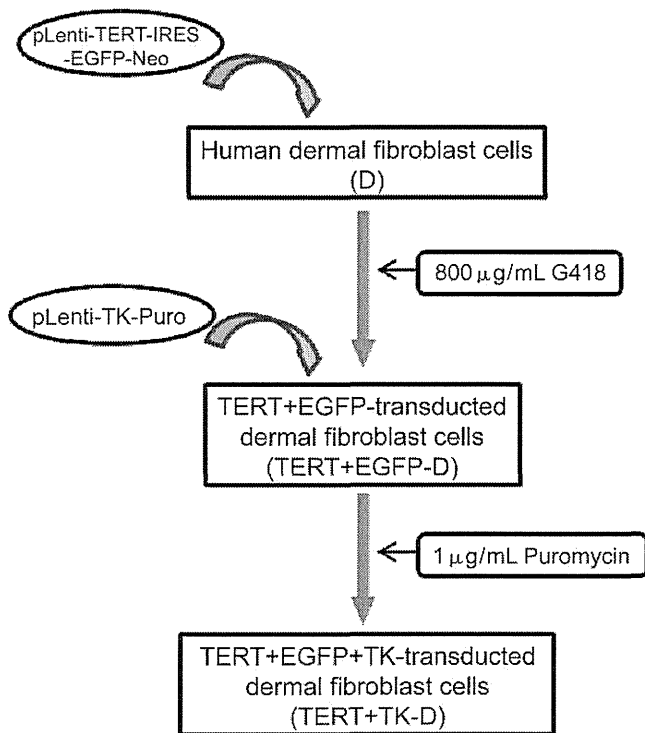


FIGURE 1. A flow chart of the development of TERT+TK-D feeder cells. TERT+TK-D feeder cells are produced in 2 steps. First, normal human dermal fibroblasts (D) are infected with lentivirus (pLenti-TERT-IRES-EGFP-Neo). After infection, selection by 800 $\mu\text{g}/\text{mL}$ G418 is performed and TERT+EGFP-transduced human dermal fibroblasts are produced. Second, TERT+EGFP-transduced human dermal fibroblasts are infected with lentivirus (pLenti-TK-Puro). After infection, selection by 1 $\mu\text{g}/\text{mL}$ puromycin is performed and TERT+EGFP+TK-transduced dermal fibroblasts (TERT+TK-D) are produced.

METHODS

Development of Genetically Modified Dermal Fibroblast Feeder Cells

As previously described,⁹ lentiviral vectors were constructed by using Gateway Technology (Invitrogen, Gaithersburg, MD). Replication-defective, self-inactivating lentiviral vectors with a phosphoglycerate kinase (PGK) promoter-neomycin resistance gene (pLentiNeo) or a PGK promoter-puromycin resistance gene (pLentiPuro) were prepared as destination vectors. The human-derived telomerase reverse transcriptase gene (TERT) and an internal ribosome entry site (IRES), enhanced green fluorescent protein gene (EGFP), were cloned into a pENTR1A vector (Invitrogen), resulting in pENTR-TERT-IRES-EGFP. The herpes simplex virus thymidine kinase gene (HSVTK) was cloned into the pENTR1A vector, resulting in pENTR-TK. LR recombination reactions were performed with the entry vectors (pENTR-TERT-IRES-EGFP or pENTR-TK) and the destination vectors (pLentiNeo or pLentiPuro) to create lentiviral expression vectors pLenti-TERT-IRES-EGFP-Neo and pLenti-TK-Puro. The lentivirus was produced by cotransfecting 293T cells with the lentiviral expression vector Plp/VSVG (encoding the Varicella-Zoster virus (VZV)-G envelope protein) and the packaging constructs pLP1 and pLP2 (Invitrogen). Concentrated lentivirus was used to infect human dermal fibroblast cells.

TERT+EGFP+TK-transduced dermal fibroblast cells were produced in 2 steps (Fig. 1). First, normal human dermal fibroblasts (KF-4009) (Kurabo, Osaka, Japan) were used for

infection with lentivirus pLenti-TERT-IRES-EGFP-Neo and selected by 800 $\mu\text{g}/\text{mL}$ G418 (Invitrogen) to produce TERT+EGFP-transduced dermal fibroblast cells. The TERT+EGFP-transduced dermal fibroblast cells then were used for infection with lentivirus pLenti-TK-Puro and selected by 1 $\mu\text{g}/\text{mL}$ puromycin (Sigma, St. Louis, MO) to produce TERT+EGFP+TK-transduced dermal fibroblast cells (TERT+TK-D). Developed TERT+TK-D cells were maintained in Fibrolife S2 cell culture medium (Lifeline Cell Technology, Walkersville, MD) supplemented with 1% penicillin-streptomycin (Invitrogen).

Ganciclovir Cytotoxicity

To evaluate the cytotoxicity of ganciclovir (GCV) (Invitrogen, San Diego, CA), TERT+TK-D cells were plated in 96-well plates at a density of 5000 cells/well. After 24 hours, the cells were treated with GCV at increasing concentrations (0, 5, 25, and 125 $\mu\text{g}/\text{mL}$) and incubated at 37°C in 5% CO₂ for 1 to 6 days. Cellular viability was measured by using the Cell Counting Kit-8 (CCK-8; Dojindo, Tokyo, Japan) every 24 hours according to the manufacturer's protocol. Background referred to the absorbance of medium alone. Control referred to the absorbance in cells not treated with GCV. The cytotoxic effect was indicated as the percentage of surviving cells.

Preparation of Feeder Layers

TERT+TK-D cells and 3T3 cells were inactivated mitotically by incubation with 8 $\mu\text{g}/\text{mL}$ mitomycin C (MMC) (Kyowa Hakko, Tokyo, Japan) for 2 hours at 37°C. The cells were washed thoroughly and reseeded in 6-well plates or type I collagen gel (Collagen Gel Culturing Kit; Nitta Gelatin, Osaka, Japan)-coated Transwell inserts (Corning, Cambridge, MA) at 0.5×10^4 cells/cm² (TERT+TK-D) or 2×10^4 cells/cm² (3T3) as the feeder layers.

Isolation of Limbal Epithelial Cells

Research corneas were obtained from the Northwest Lions Eye Bank (Seattle, WA). The endothelial cells were removed from the remaining corneal scleral rims after keratoplasty and then incubated with 2.4 U/mL Dispase solution (BD Biosciences, Bedford, MA) for 1 hour at 37°C and treated with 0.02% ethylenediaminetetraacetic acid (EDTA) solution (Nacalai Tesque, Kyoto, Japan) for 2 minutes at room temperature. The epithelial cells including the limbal zones were scraped with sterile surgical forceps. The collected cells were incubated with 0.25% trypsin-EDTA (Invitrogen, Grand Island, NY) for 15 minutes at 37°C. Obtained epithelial cells were suspended in keratinocyte culture medium (KCM) composed of Dulbecco's modified eagle medium and Ham's F12 medium (DMEM/F12, 3:1), 5% fetal bovine serum (FBS) (Invitrogen), 1 nM cholera toxin (Calbiochem, La Jolla, CA), 2 nM triiodothyronine (Takeda, Osaka, Japan), 0.4 $\mu\text{g}/\text{mL}$ hydrocortisone (Kowa, Tokyo, Japan), 1% insulin-transferrin-selenium supplement (Invitrogen), 100 U/mL penicillin, and 100 $\mu\text{g}/\text{mL}$ streptomycin (Invitrogen). Collected epithelial cells were used for a colony-forming assay or limbal epithelial cell-sheet regeneration. Our research adhered to the tenets of the Declaration of Helsinki.

Colony-Forming Assay

Primary limbal epithelial cells were seeded at a density of 1000 cells/well in 6-well plates on MMC-treated TERT+TK-D or 3T3 feeder layers and incubated for 10 to 13 days as previously described. The colonies were fixed with 10% neutral buffered

TABLE. Primers Used in Reverse Transcription-PCR

Gene		Primer Sequence, 5'→3'	Product Size, bp
HGF	Forward:	GCCTGAAAGATATCCCGACA	523
	Reverse:	TTCATGTTCTTGTCACACA	
KGF	Forward:	AGGCTCAAGTTGCACCAGGCA	495
	Reverse:	TGTGTGTCGCTCAGGGCTGGA	
EPR	Forward:	AGGAGGATGGAGATGCTCTG	498
	Reverse:	TCAGACTTGCGGCAACTCTG	
BDNF	Forward:	AACAATAAGGACGCAGACTT	222
	Reverse:	TGCAGTCTTTTTGTCTGCCG	
bFGF	Forward:	AAGAGCGACCTCACATCAAGCTA	236
	Reverse:	TACTGCCAGTTCGTTTCAGTGC	
N-cad	Forward:	CACCCAACATGTTTACAATCAACAATGAGAC	444
	Reverse:	CTGCAGCAACAGTAAGGACAAACATCCTATT	
GAPDH	Forward:	TCCAGAACATCATCCCTGCCTCTA	255
	Reverse:	TGTTGAAGTCAGAGGAGACCCTG	

formalin and stained with 1% rhodamine B (Wako, Osaka, Japan). The colony-forming efficiency (CFE) was calculated as the percentage of colonies (or colony with a diameter > 2 mm) that formed divided by the total number of viable cells seeded.

Preparation of Limbal Epithelial Cell Sheets

Primary limbal epithelial cells were inoculated on the feeder cells containing a collagen gel-coated Transwell insert at 1 to 2×10^5 cells/insert. The cells were submerged in a KCM culture for 12 days and then exposed to 25 μ g/mL GCV KCM medium as air-lifting culture for 6 to 8 days to promote epithelial stratification. For the GCV-untreated TERT+TK-D feeder cell group, epithelial cell sheets were continuously maintained in KCM medium for air-lifting culture. The medium was changed every 2 days.

Reverse Transcription-PCR and Quantitative PCR

Total RNA was extracted by using RNeasy Mini Kit (Qiagen, Valencia, CA), according to the manufacturer's instructions. Complementary DNAs (cDNAs) were synthesized from total RNA by using the first Strand cDNA Synthesis System (Origene, Rockville, MD) for PCR and quantitative PCR. The PCR procedure was as follows: initial denaturation of 94°C for 5 minutes, denaturation at 94°C for 30 seconds, extension of 60°C for 30 seconds, 72°C for 30 seconds, and a final extension

of 10 minutes at 72°C for a total of 35 cycles. Polymerase chain reaction products were run on a 2% agarose gel and scanned by using an ultraviolet gel doc. The specific primers for PCR are listed in the Table. The expressions of various genes were normalized by using glyceraldehyde-3-phosphate dehydrogenase (GAPDH) as an internal control. Quantitative PCR was carried out by using Taqman probes and the Applied Biosystems 7900 HT sequence detection system instrument (Applied Biosystems, Foster City, CA). The primers for *Anp63* (Hs00978339_m1), keratin 3 (K3) gene (Hs00365080_m1), and *GAPDH* (Hs99999905_m1) were obtained from Applied Biosystems. The cycling conditions were 10 seconds at 95°C followed by 45 two-step cycles (15 seconds at 95°C and 1 minute at 60°C). The quantification data were analyzed by using the Sequence Detection System software (Applied Biosystems) with GAPDH as an internal control. The final results are expressed as the average value of 3 experiments.

PCR Analysis of Feeder Cell Contamination

Portions of the GCV-treated and GCV-untreated TERT+TK-D feeder cell-cocultured epithelial sheets were harvested. Genome DNAs were extracted with QIAamp DNA Mini Kit (Qiagen) according to the manufacturer's instructions. The long terminal repeat (LTR) sequence, which is specific to the lentivirus vector, was integrated into the TERT+TK-D feeder cells. The following primers were used to target the LTR sequence: forward primer, 5'-AAGGGCTAATTCCTCCCAA-3', and reverse primer, 5'-TGCCTCGAGAGAGCTCTGGTTT-3', with the GAPDH sequence as an internal control. The PCR reaction was performed as previously described.

Histology and Immunofluorescence Staining

Harvested cell sheets were embedded in Tissue-Tek OCT compound (Sakura Finechemical Co., Tokyo, Japan) for hematoxylin-eosin and immunofluorescence staining. Hematoxylin-eosin staining was performed according to standard protocols for histologic examination. For immunofluorescence staining, sections and cells were fixed in 4% paraformaldehyde at 4°C for 30 minutes followed by blocking in 4% nonfat milk and 0.3% Triton X-100 in phosphate-buffered saline (PBS) for 1 hour at room temperature. The samples then were incubated overnight at 4°C with the following primary antibodies: anti-K3 (AE5) (1:100; Progen Biotechnik, Heidelberg, Germany), anti-keratin12 (1:100; Santa Cruz Biotechnology, Santa Cruz, CA), and anti-P63 (4A4) (1:100; Santa Cruz Biotechnology). After

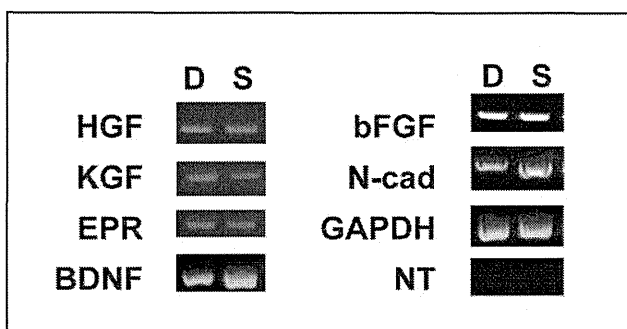


FIGURE 2. Comparison of gene expression in in vitro cultured dermal fibroblasts and in corneal stromal fibroblasts by reverse transcription-PCR. Similar to corneal stromal cells, dermal fibroblasts express many factors to maintain stem/progenitor cells and epithelial cell growth. D, dermal fibroblasts; S, corneal stromal fibroblasts; NT, no reverse transcriptase.

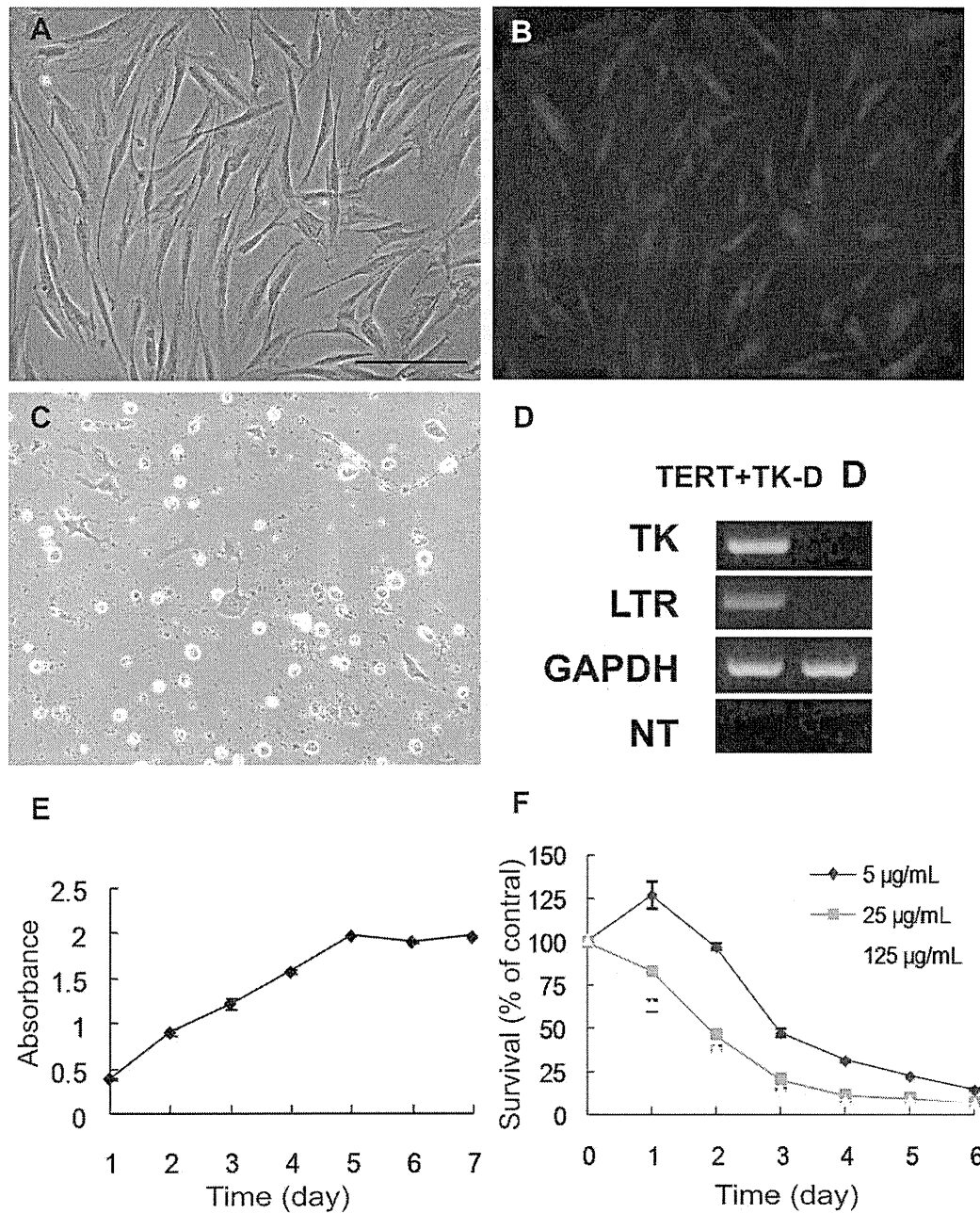


FIGURE 3. The characteristics of TERT+TK-D feeder cells. (A) The cell morphology of TERT+EGFP+TK-transduced human dermal fibroblast cells (TERT+TK-D). (B) TERT+TK-D feeder cells expressed green fluorescence under ultraviolet illumination. (C) The TERT+TK-D feeder cells are eliminated at day 6 by 25 µg/mL GCV. (D) The TK and LTR sequence are detected in TERT+TK-D feeder cells by PCR analysis, while dermal fibroblasts are not detected. (E) The cell growth curve of the TERT+TK-D feeder cells. (F) The sensitivity of the TERT+TK-D cells to a GCV assay shows that the minimal lethal dose of GCV is 25 µg/mL. TK, herpes simplex virus thymidine kinase. Scale bar: 200 µm.

washing with PBS, the samples were incubated for 1 hour with Alexa 568 or FITC-conjugated secondary antibody (1:200; Invitrogen) and finally counterstained with 4',6-diamidino-2-phenylindole (Sigma) and viewed under a Zeiss fluorescence microscopy (Axiovert 200M; Carl Zeiss Jena GmbH, Jena Germany). The same concentration of corresponding normal, nonspecific IgG was used as a negative control.

Statistics

Statistical analysis was performed by using SPSS 16.0 software (SPSS, Inc., Chicago, IL). Data were analyzed by using an

independent samples *t*-test; $P < 0.05$ was considered statistically significant.

RESULTS

Gene Expression Pattern of Human Dermal Fibroblasts

The gene expression pattern of dermal fibroblasts was similar to that of the corneal stromal fibroblasts (Fig. 2). They both expressed cytokine hepatocyte growth factor (HGF), keratino-

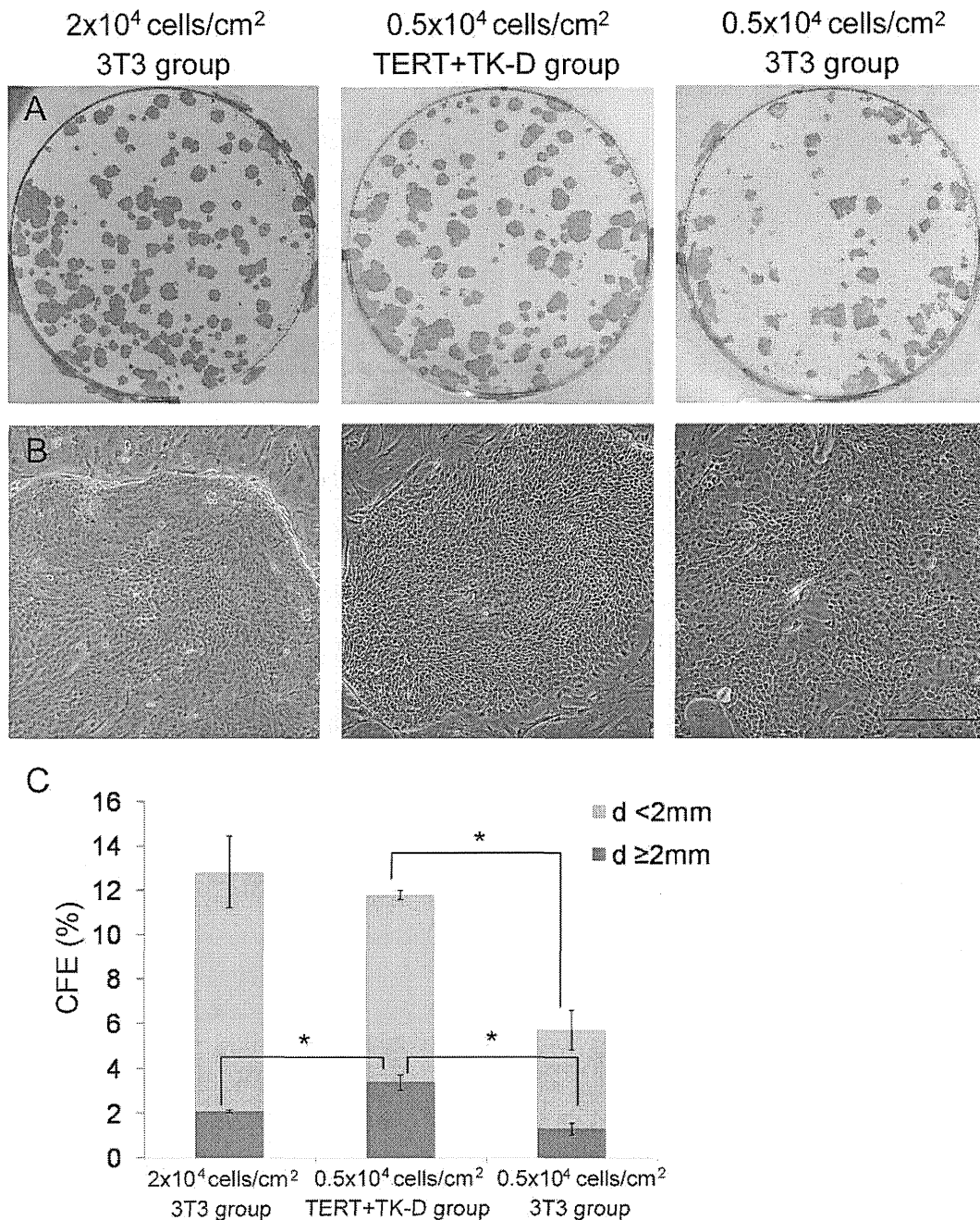


FIGURE 4. Colony-forming assay. Primary limbal epithelial cells form typical cell colonies on the genetically modified dermal fibroblast (TERT+TK-D) and 3T3 fibroblast feeder layers after 10 to 13 days' culture. (A, B) The TERT+TK-D group shows more colony formation and typical epithelial cell morphology, compared with the 3T3 cell group at the same density and 2×10^4 cells/cm² 3T3 cell group. (C) CFE analysis shows that the TERT+TK-D group forms more large colonies (diameter > 2 mm) and has a CFE similar to that of the 2×10^4 cells/cm² 3T3 cell group. Scale bar: 200 μ m. * $P < 0.05$.

cyte growth factor (KGF), epiregulin (EPR), brain-derived neurotrophic factor (BDNF), fibroblast growth factor 2 (bFGF), and adhesion molecule N-cadherin (N-cad).

Characteristics of TERT+TK-D Feeder Cells

After transducing the human-derived *TERT* gene, the *EGFP* gene, and the *HSVTK* gene, the TERT+TK-D cells were developed. To test the immortalization ability of TERT+TK-D cells, genetically modified cells were continuously passaged for 6 months (>50 generations). After multiple passages, the cells still exhibited a fibroblast-like morphology like primary human

dermal fibroblast cells (Fig. 3A), expressed green fluorescence under ultraviolet illumination (Fig. 3B), and were sensitive to GCV (Fig. 3C). Reverse transcription-PCR revealed expression of the *TK* gene and lentivirus vector special LTR sequence in TERT+TK-D cells but not in normal human dermal fibroblast cells (Fig. 3D). TERT+TK-D cells passaged over the long term, exceeding the normal lifespan, showed a vigorous ability to divide (Fig. 3E). A GCV cytotoxicity assay showed that the drug killed the TERT+TK-D cells in a dose-dependent manner. In the 25 μ g/mL-GCV group, almost all cells were positive for apoptosis in 6 days (Fig. 3F).

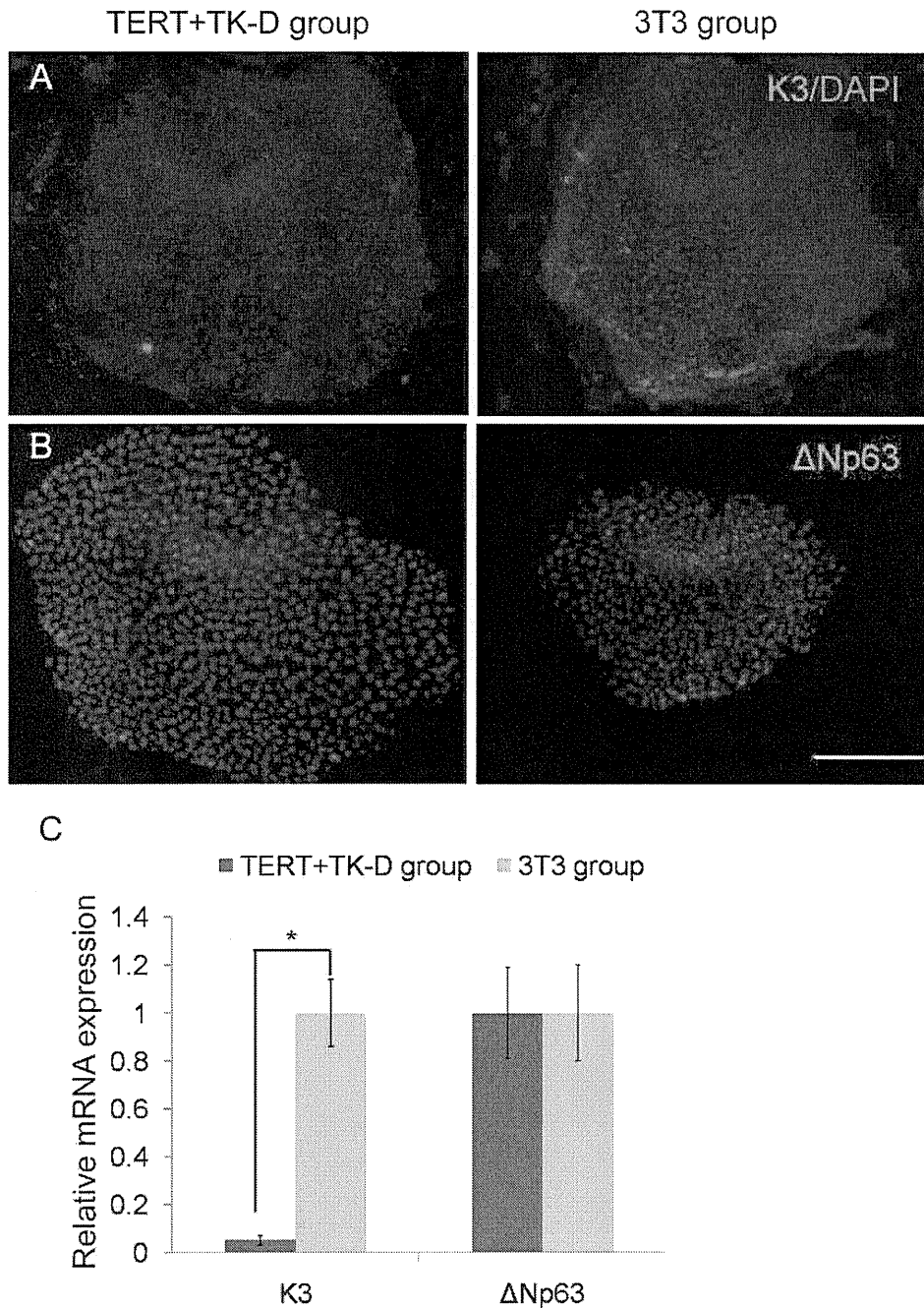


FIGURE 5. Characterization of limbal epithelial stem/progenitor colonies. (A) Compared with the 3T3 feeder cell group, coculture of limbal epithelial cells in the TERT+TK-D feeder cells group shows lower positive staining of differentiated corneal epithelial cell marker K3. (B) There is no significant difference in expression of limbal stem/progenitor cell marker Δ Np63 and (C) quantitative analysis of mRNA transcripts. Scale bar, 200 μ m. * $P < 0.05$.

Colony-Forming Assay and Characterization

To compare the ability of TERT+TK-D and 3T3 cells to support colony formation, 3T3 feeder cells were divided into 2 groups at a density of 2×10^4 cells/cm² (gold standard density) and 0.5×10^4 cells/cm². At 10 to 13 days, the primary limbal stem/progenitor cells formed typical cell colonies in all groups (Figs. 4A, 4B). The TERT+TK-D group (CFE, $11.77 \pm 0.21\%$) formed more colonies and typical epithelial cell morphology, in comparison with the 3T3 cell group with the same density (CFE, $5.7 \pm 0.89\%$) ($P < 0.001$), and the same as the 2×10^4 cells/cm² 3T3 cell group (CFE, $12.8 \pm 1.61\%$) ($P = 0.332$).

More large colonies (diameter > 2 mm) formed in the TERT+TK-D group (diameter ≥ 2 mm; CFE, $3.37 \pm 0.35\%$) than in the 0.5×10^4 cells/cm² 3T3 cell group (diameter ≥ 2 mm; CFE, $1.3 \pm 0.26\%$) ($P = 0.01$) and in the 2×10^4 cells/cm² 3T3 cell group (diameter ≥ 2 mm, CFE, $2.07 \pm 0.06\%$) ($P = 0.03$) (Fig. 4C).

On the ninth day of culture, the limbal epithelial cell colonies were fixed and stained for immunofluorescence with corneal epithelium differentiation marker K3 and putative limbal stem/progenitor cell marker Δ Np63. Colonies were selected for measurement of the transcript levels of K3 and Δ Np63 by using quantitative real-time PCR analysis. The

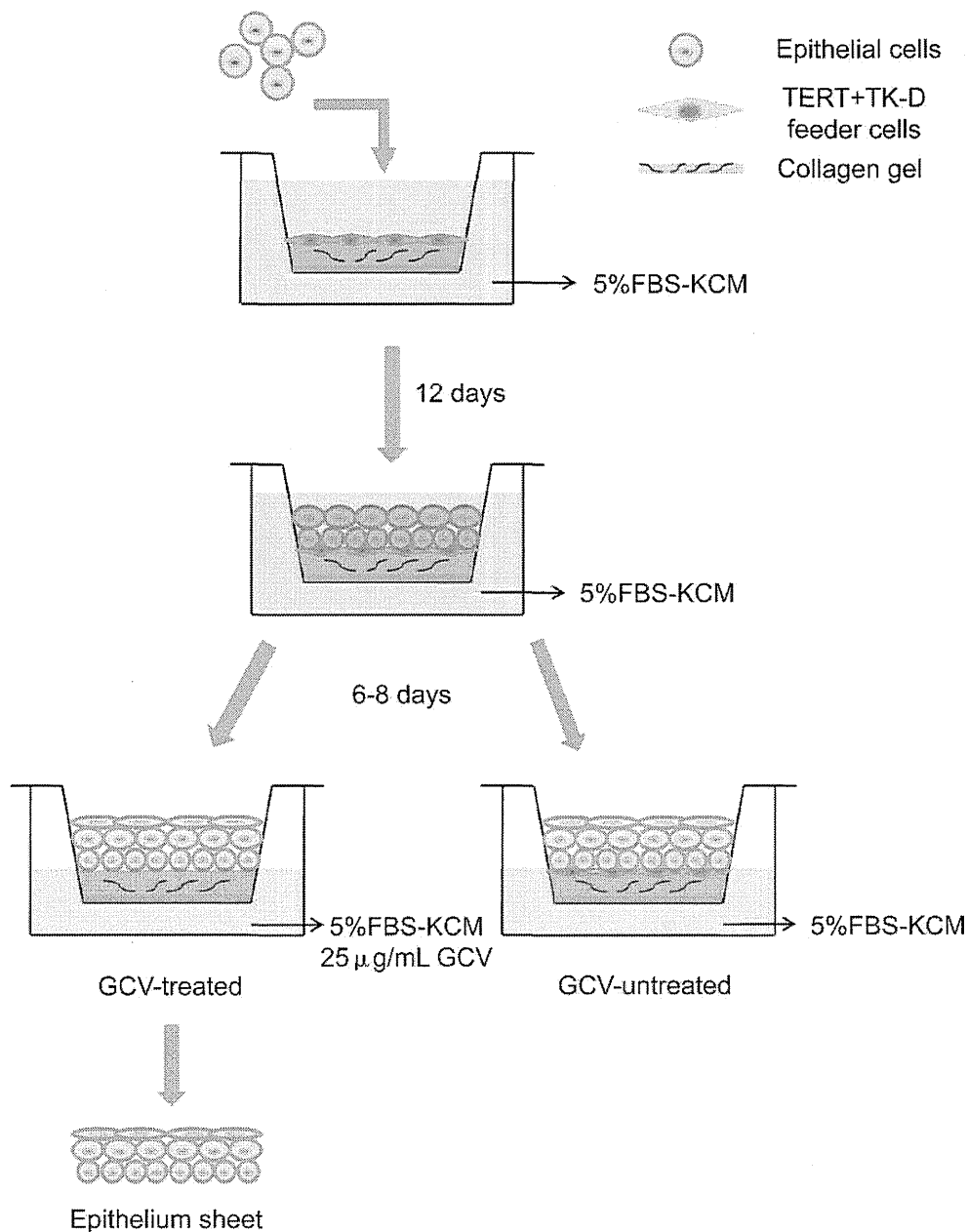


FIGURE 6. A flow chart of the procedures for harvesting GCV-treated and GCV-untreated TERT+TK-D feeder cell-cocultured epithelial cell sheets. Primary limbal epithelial cells are inoculated on TERT+TK-D feeder cells containing a collagen gel-coated Transwell insert. The cells are submerged in a culture of 5% FBS-KCM for 12 days and then undergo the process of air-lifting for 6 days to promote epithelial stratification. For the GCV-treated group, 25 µg/mL of GCV is added to the medium during the last 6 to 8 days to kill the TERT+TK-D feeder cells. The harvested epithelium sheet after eliminating feeder cell layer can be easily peeled by using surgical forceps for transplantation or immunohistochemistry assay.

epithelial cells in both groups were positive for expression of K3 and Δ Np63 marker (Figs. 5A, 5B), while limbal epithelial cells in the TERT+TK-D group had less positive staining of K3 than the 3T3 group. Real-time PCR (Fig. 5C) confirmed that expression of K3 in the epithelial cells in the TERT+TK-D group was significantly lower ($P=0.01$) than in the cells in the 3T3 group. However, no significant difference in Δ Np63 expression ($P=0.982$) was detected.

PCR Analysis of Feeder Cell Contamination

The flow chart shows the procedures for harvesting GCV-treated and GCV-untreated TERT+TK-D feeder cell-cocultured epithelial cell sheets (Fig. 6). Limbal epithelial cells cocultured

with TERT+TK-D feeder layers were submerged in a KCM culture for 12 days and then submitted to a process referred to as air-lifting for 6 to 8 days to promote epithelial stratification. The epithelial cell sheets of the GCV-treated TERT+TK-D group were treated with 25 µg/mL GCV during the final 6 to 8 days to eliminate the feeder cells, while the epithelial cell sheets of the GCV-untreated TERT+TK-D feeder cell group were continuously maintained in KCM medium for air-lifting culture. Genome DNAs were extracted from GCV-treated and GCV-untreated TERT+TK-D feeder cell-cocultured epithelial cell sheets. Polymerase chain reaction analysis was performed to detect the LTR sequence, which is specific to the lentiviral vector and was integrated into the lentivirus-infected cells. Both cell sheets were positive for expression of the internal

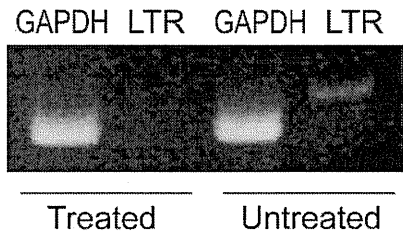


FIGURE 7. PCR analysis of the LTR sequence. PCR is performed against an LTR sequence of lentiviral vector integrated into genetically modified feeder cells and a GAPDH sequence as a positive control. The LTR sequence is detected in the GCV-untreated TERT+TK-D feeder cell-cocultured epithelial cell sheet but not in the GCV-treated cocultured cell sheet.

control *GAPDH* gene, but the LTR sequence was detected only in the GCV-untreated epithelial cell sheets. In the GCV-treated epithelial cell sheets, the lentiviral vector special sequence LTR was not detected (Fig. 7).

Characterization of Cultured Limbal Epithelial Cell Sheets

Limbal stem/progenitor cells were cocultured with TERT+TK-D or 3T3 feeder cells to form epithelial cell sheets. The cells were submerged in a culture in KCM for 12 days and then underwent air-lifting in 25 $\mu\text{g}/\text{mL}$ GCV KCM medium for 6 to 8 days to promote epithelial stratification. After 2 to 3 weeks' culture, both groups formed 4 to 5 layers of epithelial cell sheets (Fig. 8A). Limbal epithelial cells and 3T3 feeder cells grew well under 25 $\mu\text{g}/\text{mL}$ GCV condition, which is a safety concentration for normal cells, whereas TERT+TK-D feeder cells in the TERT+TK-D group diminished in 6 days by ganciclovir treatment. Immunofluorescence analyses showed that the cell sheets in both groups expressed corneal epithelial

cell differentiation marker K3¹⁰ (Fig. 8B), putative corneal epithelial stem cell marker ΔNp63 ¹¹ (Fig. 8C), and corneal epithelium specific marker K12¹² (Fig. 8D). Compared with the 3T3 group, the epithelial cell sheets in the TERT+TK-D group had lower expression of K3 and higher expression of ΔNp63 in the basal and wing cells. No difference in K12 staining was detected.

DISCUSSION

Our results confirmed that genetically modified, immortalized, visualized, eliminable human dermal fibroblast feeder cells maintained the ability to support limbal stem/progenitor cell growth and differentiation and prevented feeder cell self-contamination.

To avoid the use of animal-derived feeder cells, human-derived feeder cells, such as mesenchymal stem cells,^{13,14} corneal stromal fibroblasts,^{15,16} and dermal fibroblasts⁷ have been studied widely as substitutes for 3T3 fibroblasts. Oie et al.⁷ report that dermal fibroblasts have been used successfully in oral mucosal epithelial cell-sheet culture for ocular surface reconstruction. Sharma et al.⁸ have compared human dermal fibroblasts and mesenchymal stem cells, with 3T3 fibroblasts, as feeder layers for the vivo expansion of human limbal and oral epithelium. The investigators have found that dermal fibroblasts are comparable to 3T3 fibroblasts and superior to mesenchymal stem cells in the cultivation of epithelium. In the current study, we found that the gene expression pattern of dermal fibroblasts was similar to that of corneal stromal fibroblasts. Dermal fibroblasts expressed many genes required for maintenance and proliferation of limbal epithelial cells like corneal stromal fibroblast cells,¹⁷ that is, HGF,¹⁸ KGF,¹⁸ EPR,¹⁹ BDNF,²⁰ bFGF,²¹ and N-cad.²² In a preliminary experiment, we also compared human dermal fibroblasts with corneal stromal fibroblasts and found that the CFE of the limbal stem/progenitor cells cocultured on dermal fibroblasts was signifi-

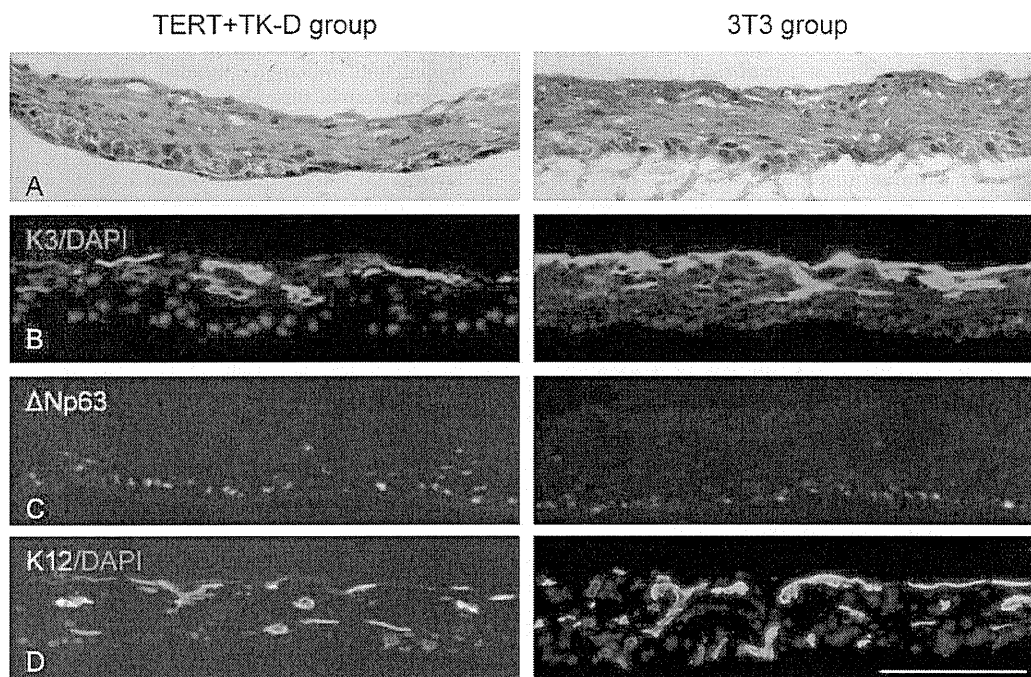


FIGURE 8. Characterization of cultured limbal epithelial cell sheets. (A) Both the TERT+TK-D cells and 3T3 cells support stratification of limbal epithelial cells after 2 to 3 weeks' culture. (A) The TERT+TK-D cells support formation of 4 to 5 layers of epithelium and 3T3 feeder cells. (B) Moreover, the epithelial cell sheet cocultured with the TERT+TK-D feeder cells has lower expression of K3 and (C) higher expression of ΔNp63 in both basal cells and wing cells. (D) The K12 staining does not differ significantly. Scale bar: 200 μm .

cantly higher than on corneal stromal fibroblasts (data not shown). Therefore, human dermal fibroblasts could be a promising alternative to 3T3 fibroblasts.

To use human dermal fibroblasts as feeder cells, the *hTERT* gene²³ was transduced into cells to prevent replicative senescence. In the current study, immortalized dermal fibroblast cells were maintained for more than 6 months (over 50 generations in *in vitro* culture). After extended continuous passaging, the cells still showed a vigorous ability to divide, visible under ultraviolet illumination, and were killed by GCV. Immortalization treatment greatly facilitates cellular storage and access, reducing the cost of primary culture and decreasing the risk of repeats using lentivirus. The *TK* gene²⁴ also was transduced into the hTERT and EGFP-transduced dermal fibroblast cells to eliminate unknown infections and contamination from xenogeneic feeder cells. In the current study, GCV-treated epithelial sheets, when cocultured with TERT+TK-D feeder cells, were uncontaminated by feeder cells, compared with GCV-untreated epithelial sheets, which were cultured under the same conditions by detecting the ITR sequence. The eliminable feeder cells are convenient for use whether they are mixed or in a contact culture system when feeder cells are needed. Moreover, the eliminable character of feeder cells also reduced the unknown risks induced by the transduced exogenous genes and increased the safety of using genetically modified cells.

Sharma et al.⁸ have compared normal human dermal fibroblasts with 3T3 feeder cells for the expansion of limbal epithelial cells. They found that colony-forming efficiency and stem cell marker expression of limbal epithelial cells on dermal fibroblasts are comparable to cells grown on 3T3 feeder cells. Our experiment showed that *TERT*, *EGFP*, and *TK*-transduced dermal fibroblast cells maintained the fibroblast morphology and vigorous dividing ability of the early-generation normal dermal fibroblast cells. The gene-modified dermal fibroblasts also maintained the same ability of supporting limbal epithelial cell growth as nonmodified dermal fibroblast cells. The epithelial cell sheets stratified into 4 to 5 layers on both the TERT+TK-D and 3T3 feeder layers. The CFE of the limbal stem/progenitor cells in the TERT+TK-D group was similar to that of the standard-density 3T3 group as reported previously.⁸ Interestingly, the TERT+TK-D group formed more large colonies (diameter ≥ 2 mm) than the standard-density 3T3 group, and the CFE was higher than that of the same-density 3T3 group. Moreover, immunohistochemistry and real-time PCR analyses found that the TERT+TK-D group had lower expression of the corneal epithelium differentiation marker K3, compared with the 3T3 group, and the TERT+TK-D feeder cells better maintained the undifferentiated state of the epithelium.

Bullock et al.²⁵ have recently reported using human dermal fibroblasts to develop xenobiotic-free human skin keratinocytes. Rodriguez-Piza et al.²⁶ have successfully derived primary cultures of human dermal fibroblasts under xeno-free conditions and showed that they can be used as both the cell source for induced pluripotent stem cell generation and as autologous feeder cells to support their growth. In the current study, we focused only on the development, characterization, and feeder effect of the genetically modified dermal fibroblasts. The current results suggest that genetically modified dermal fibroblasts maintain the feeder effect and become more convenient, economical, and safer. Future research should be performed under xeno-free conditions by substituting commonly used ingredients with products of human origin, such as human serum instead of FBS.²⁷ Meanwhile, the use of genetically modified dermal fibroblasts should be investigated widely in other regenerative treatments, for example, in coculture with oral epithelial cells or keratinocytes.

In summary, we developed genetically modified, labeled, immortalized, and eliminable human dermal fibroblast feeder cells and confirmed that their use is effective and safe. These findings suggest that genetically modified feeder cells could be a promising alternative feeder for human regeneration medicine.

Acknowledgments

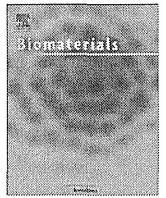
Supported partially by Grant-in-Aid for Scientific Research (TD). The authors alone are responsible for the content and writing of the paper.

Disclosure: Y. Li, None; T. Inoue, P; F. Takamatsu, None; N. Maeda, None; Y. Ohashi, None; K. Nishida, None

References

- Rama P, Matuska S, Paganoni G, Spinelli A, De Luca M, Pellegrini G. Limbal stem-cell therapy and long-term corneal regeneration. *New Engl J Med*. 2010;363:147-155.
- Koizumi N, Inatomi T, Suzuki T, Sotozono C, Kinoshita S. Cultivated corneal epithelial stem cell transplantation in ocular surface disorders. *Ophthalmology*. 2001;108:1569-1574.
- Nishida K, Yamato M, Hayashida Y, et al. Corneal reconstruction with tissue-engineered cell sheets composed of autologous oral mucosal epithelium. *New Engl J Med*. 2004;351:1187-1196.
- Takeda K, Nakamura T, Inatomi T, Sotozono C, Watanabe A, Kinoshita S. Ocular surface reconstruction using the combination of autologous cultivated oral mucosal epithelial transplantation and eyelid surgery for severe ocular surface disease. *Am J Ophthalmol*. 2011;152:195-201.e191.
- Martin MJ, Muotri A, Gage F, Varki A. Human embryonic stem cells express an immunogenic nonhuman sialic acid. *Nature Med*. 2005;11:228-232.
- Heiskanen A, Satomaa T, Tiitinen S, et al. N-glycolylneuraminic acid xenotigen contamination of human embryonic and mesenchymal stem cells is substantially reversible. *Stem Cells*. 2007;25:197-202.
- Oie Y, Hayashi R, Takagi R, et al. A novel method of culturing human oral mucosal epithelial cell sheet using post-mitotic human dermal fibroblast feeder cells and modified keratinocyte culture medium for ocular surface reconstruction. *Br J Ophthalmol*. 2010;94:1244-1250.
- Sharma SM, Fuchsluger T, Ahmad S, et al. Comparative analysis of human-derived feeder layers with 3T3 fibroblasts for the *ex vivo* expansion of human limbal and oral epithelium. *Stem Cell Rev*. 2012;8:696-705.
- Takamatsu F, Inoue T, Li Y, et al. New culture technique of human eliminable feeder-assisted target cell sheet production. *Biochem Biophys Res Commun*. 2010;399:373-378.
- Robertson DM, Li L, Fisher S, et al. Characterization of growth and differentiation in a telomerase-immortalized human corneal epithelial cell line. *Invest Ophthalmol Vis Sci*. 2005;46:470-478.
- Pellegrini G, Dellambra E, Golisano O, et al. p63 identifies keratinocyte stem cells. *Proc Natl Acad Sci U S A*. 2001;98:3156-3161.
- Chen WYW, Mui MM, Kao WWY, Liu CY, Tseng SCG. Conjunctival epithelial-cells do not transdifferentiate in organotypic cultures: expression of K12 keratin is restricted to corneal epithelium. *Curr Eye Res*. 1994;13:765-778.
- Omoto M, Miyashita H, Shimmura S, et al. The use of human mesenchymal stem cell-derived feeder cells for the cultivation of transplantable epithelial sheets. *Invest Ophthalmol Vis Sci*. 2009;50:2109-2115.
- Havasi PNM, Soleimani M, Bakhshandeh B, Parivar K. Mesenchymal stem cells as an appropriate feeder layer for

- prolonged in vitro culture of human induced pluripotent stem cells. *Mol Biol Rep.* 2013;40:3023-3031.
15. Chen SY, Hayashida Y, Chen MY, Xie HT, Tseng SC. A new isolation method of human limbal progenitor cells by maintaining close association with their niche cells. *Tissue Eng Part C Methods.* 2011;17:537-548.
 16. Zhang XM, Sun HM, Li XR, Yuan XY, Zhang L, Zhao SZ. Utilization of human limbal mesenchymal cells as feeder layers for human limbal stem cells cultured on amniotic membrane. *J Tissue Eng Regen Med.* 2010;4:38-44.
 17. Wilson SE, Liu JJ, Mohan RR. Stromal-epithelial interactions in the cornea. *Prog Retin Eye Res.* 1999;18:293-309.
 18. Yu FSX, Yin J, Xu KP, Huang J. Growth factors and corneal epithelial wound healing. *Brain Res Bull.* 2010;81:229-235.
 19. Morita S, Shirakata Y, Shiraishi A, et al. Human corneal epithelial cell proliferation by epiregulin and its cross-induction by other EGF family members. *Mol Vis.* 2007;13:2119-2128.
 20. You LT, Kruse FE, Volcker HE. Neurotrophic factors in the human cornea. *Invest Ophthalmol Vis Sci.* 2000;41:692-702.
 21. Yanai R, Yamada N, Kugimiya N, Inui M, Nishida T. Mitogenic and antiapoptotic effects of various growth factors on human corneal fibroblasts. *Invest Ophthalmol Vis Sci.* 2002;43:2122-2126.
 22. Hayashi R, Yamato M, Sugiyama H, et al. N-cadherin is expressed by putative stem/progenitor cells and melanocytes in the human limbal epithelial stem cell niche. *Stem Cells.* 2007;25:289-296.
 23. Bodnar AG, Ouellette M, Frolkis M, et al. Extension of life-span by introduction of telomerase into normal human cells. *Science.* 1998;279:349-352.
 24. Qiao J, Doubrovin M, Sauter BV, et al. Tumor-specific transcriptional targeting of suicide gene therapy. *Gene Ther.* 2002;9:168-175.
 25. Bullock AJ, Higham MC, Macneil S. Use of human fibroblasts in the development of a xenobiotic-free culture and delivery system for human keratinocytes. *Tissue Eng.* 2006;12:245-255.
 26. Rodriguez-Piza I, Richaud-Patin Y, Vassena R, et al. Reprogramming of human fibroblasts to induced pluripotent stem cells under xeno-free conditions. *Stem Cells.* 2010;28:36-44.
 27. Nakamura T, Inatomi T, Sotozono C, et al. Transplantation of autologous serum-derived cultivated corneal epithelial equivalents for the treatment of severe ocular surface disease. *Ophthalmology.* 2006;113:1765-1772.



Corneal regeneration by transplantation of corneal epithelial cell sheets fabricated with automated cell culture system in rabbit model



Toyoshige Kobayashi^{a,b}, Kazutoshi Kan^a, Kohji Nishida^c, Masayuki Yamato^b, Teruo Okano^{b,*}

^a Central Research Laboratory, Hitachi, Ltd., 2520 Akanuma, Hiki-gun, Hatoyama-machi, Saitama 350-0395, Japan

^b Institute of Advanced Biomedical Engineering and Science, Tokyo Women's Medical University, TWIns, 8-1 Kawada-cho, Shinjuku-ku, Tokyo 162-8666, Japan

^c Department of Ophthalmology, Osaka University Medical School, 2-2 Yamadaoka, Suita-shi, Osaka 565-0871, Japan

ARTICLE INFO

Article history:

Received 21 June 2013

Accepted 19 July 2013

Available online 23 August 2013

Keywords:

Cell sheet engineering
Automatic cell culture system
Cell cartridge
Corneal epithelial cell
Cell sheet transportation
Cell sheet transplantation

ABSTRACT

We have performed clinical applications of cell sheet-based regenerative medicine with human patients in several fields. In order to achieve the mass production of transplantable cell sheets, we have developed automated cell culture systems. Here, we report an automated robotic system utilizing a cell culture vessel, cell cartridge. The cell cartridge had two rooms for epithelial cells and feeder layer cells separating by porous membrane on which a temperature-responsive polymer was covalently immobilized. After pouring cells into this robotic system, cell seeding, medium change, and microscopic examination during culture were automatically performed according to the computer program. Transplantable corneal epithelial cell sheets were successfully fabricated in cell cartridges with this robotic system. Then, fabricated cell sheets were transplanted onto ocular surfaces of rabbit limbal epithelial stem cell deficiency model after 6-h transportation using a portable homothermal container to keep inner temperature at 36 °C. Within one week after transplantation, normal corneal epithelium was successfully regenerated. This automatic cell culture system would be useful for industrialization of tissue-engineered products for regenerative medicine.

© 2013 Elsevier Ltd. All rights reserved.

1. Introduction

Recently, tissue engineering and regenerative medicine have become the focus of public attention, and some successful outcomes in the clinical settings have been reported. We have developed cell sheet-based regenerative medicine utilizing temperature-responsive culture surfaces [1–6]. By utilizing fabricated carrier-free cell sheets, we have successfully performed the clinical applications to treat human patients in skin [7], cornea [8,9], esophagus [10,11], heart [12], periodontal tissue [13], and knee cartridge [14].

In the clinical research, cell culture to fabricate transplantable cell sheets was manually performed in clean rooms of cell processing facilities according to the regulation of Good Manufacturing Practice (GMP) [15]. Therefore, the production cost is inevitably high. In particular, autologous tissue-engineered products are pretty expensive due to the small production. It has been pointed out that drastic reduction of the manufacturing costs should be

necessary to provide these tissue-engineered products to many patients and establish regenerative medicine as a general treatment [16–18]. Therefore, a series of new technology would be necessary to support manufacturing processes from isolation of cells from tissues to shipping inspection of the final products [19,20]. For example, in order to improve the efficiency of cell culture process, the development of an automated cell culture system (ACCS) has been promoted [21].

So far, ACCSs which handle conventional open culture vessels with robotic arms have been reported [22–25]. To minimize the possibility of bacterial and/or viral contamination, ACCSs inevitably need special air-conditioning units with high-efficiency particle arrester (HEPA) filters to use open culture vessels. Closed culture vessels connected to closed liquid circuits can reduce the size of ACCS by eliminating bulky air-conditioning units and robotic arms. For example, an ACCS using mono-layered closed culture vessels connected to a closed circuit was reported [26]. However, typical culture conditions for epithelial cells employ cell culture inserts and feeder layer cells [8–10]. Therefore, a closed culture vessel having two separate rooms and more complex closed circuits might be needed in these cases.

* Corresponding author. Fax: +81 3 3359 6046.

E-mail address: tokano@abmes.twmu.ac.jp (T. Okano).

2. Materials and methods

2.1. Cell culture

The animals were treated in accordance with experimental procedures approved by the Committees for Animal Research of Tokyo Women's Medical University and of Osaka University Medical School. Corneal limbus was excised from eyes of Japanese White rabbits by scissors, then treated with 200 U/mL of dispase II (Godo Shusei, Tokyo, Japan) in Dulbecco's modified Eagle's medium (Sigma, St. Louis, MO) at 37 °C for 1 h. Epithelium was peeled off under a dissecting microscope, and cut into small pieces by scissors. These tissues were treated with 0.25% trypsin–0.1% ethylenediamine tetraacetic acid solution (GIBCO–Invitrogen, Carlsbad, CA) for 20 min at 37 °C, to scatter the epithelial cells. Disaggregated cells were suspended in a keratinocyte culture medium (KCM) composed of a basal mixture of 3 parts Dulbecco's modified Eagle's medium and 1 part nutrient mixture F-12 Ham (Sigma), and supplemented with 2 nM triiodothyronine (Wako Pure Chemicals, Osaka, Japan), 5 µg/mL transferrin (GIBCO–Invitrogen), 5 µg/mL insulin (Eli Lilly, Indianapolis, IN), 10 ng/mL epidermal growth factor (Invitrogen), 0.4 µg/mL hydrocortisone (Kowa Pharmaceutical, Tokyo, Japan), 1 nM cholera toxin (List Biological Laboratories, Campbell, CA), 1% penicillin–streptomycin (Invitrogen), and 5% fetal bovine serum (Moregate BioTech, Queensland, Australia) [27]. The rate of viable cells was obtained by Trypan blue exclusion test on a hemocytometer under a phase-contrast microscope (TE2000; Nikon, Tokyo, Japan). To evaluate putative progenitor cell populations in the cells, colony-forming assays (CFA) were performed. The cells were seeded at the density of 200 cells/35-mm well, and cultured with mitomycin C (MMC)-treated NIH/3T3 feeder cells seeded at the density of 2.0×10^4 cells/cm². After 2 weeks, the number of colonies was counted under a microscope.

2.2. Instrumentation

2.2.1. Cell culture vessel

In the present study, we used new culture vessels, cell cartridge (Fig. 1A) [28]. The cell cartridge had two rooms for epithelial cells and feeder layer cells separated by the microporous (0.4 µm) film on which a temperature-responsive polymer, poly(*N*-isopropylacrylamide) was covalently immobilized (Fig. 1B), and were connected to closed circuits. The lower gas permeable film was treated by O₂ plasma to improve cell adhesion. Corneal epithelial cells and MMC-treated 3T3 cells were cultured in an upper and lower culture rooms, respectively.

2.2.2. Automated cell culture system

A prototype of the automated cell culture system was developed to perform cell seeding, medium change, cell culture, and microscopic monitoring of cells according to computer programs. Maximum three cell cartridges were cultured in the ACCS at one time. The ACCS had two small handling manipulators. One handled cell cartridges, the other was used only when cells were seeded into cell cartridges.

2.3. Transportation

All the cell cartridges were sealed with Parafilm (Pechiney Plastic Packaging, Chicago, IL) to avoid pouring of culture medium, packed within homothermal portable containers developed for cell sheet transportation (Hitachi Transport System, Tokyo, Japan) [29], and transported from Hitachi Central Research Laboratory (Saitama, Japan) to Osaka University Medical School (Osaka, Japan) by car and train. Temperature was continuously monitored with temperature sensors (T&D Corp., Nagano, Japan) during transportation.

2.4. Transplantation

Tissue-engineered cell sheets fabricated from cornea limbal epithelial cells were autologously transplanted onto keratectomized ocular surfaces of a rabbit limbal stem cell deficiency model surgically prepared 2 weeks before transplantation. Keratectomy was used to excise the entire corneal surface, including the limbus and the conjunctival tissue within 5 mm of the limbus, completely removing the corneal and limbal epithelium and exposing the stroma [8,30]. Six rabbits were used for epithelial cell sheet transplantation ($n = 3$) and control without cell sheet transplantation ($n = 3$). After two weeks of keratectomy, conjunctival scar tissue with some neovascularization covered the entire corneal stromal surface, including severe corneal opacity. Before cell sheet transplantation, the conjunctivalized ocular surface was surgically removed to reexpose the native transparent corneal stroma. Then, transplantable cell sheets fabricated in cell cartridges were harvested by temperature reduction (20 °C, 5% CO₂, 30 min) and transferred to a polyvinylidene difluoride (PVDF) support membrane (23 mm in diameter with a 16-mm hole in the center) and placed over the transparent stromal bed immediately. A part of corneal epithelial cell sheets was cut and processed into paraffin-embedded sections respectively. Within 5 min, the cell sheets spontaneously produced stable attachment to the stroma, and PVDF membranes were removed with scissors. For healing protection, the corneal surface was finally covered with a soft contact lens, and a tarsorrhaphy was performed. Antibiotics (0.3% ofloxacin) and steroids (0.1% betamethasone) were topically applied three times a day after transplantation. One

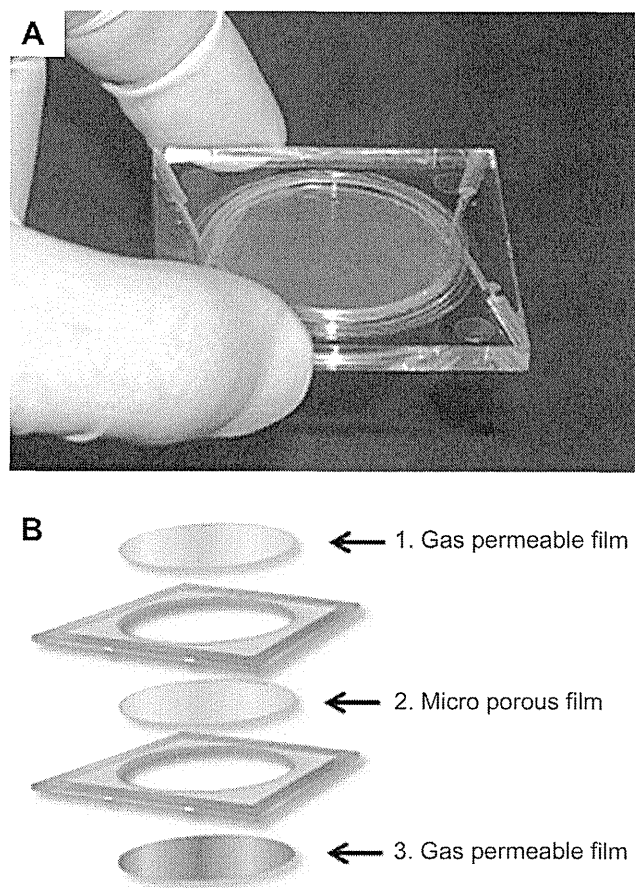


Fig. 1. A new culture vessel called cell cartridge. A, The slanting front view of the cell cartridge. B, Its inner structure. The cell cartridge had two rooms for epithelial cells and feeder layer cells separated by the microporous (0.4 µm) film on which a temperature-responsive polymer, poly(*N*-isopropylacrylamide) was covalently immobilized. The size was 46 × 46 × 4 mm (WDH).

week after surgery, rabbits were sacrificed. The operated eyes were enucleated, and the each cornea of operated eyes was cut into three sections and processed into paraffin-embedded sections, respectively.

2.5. Histology

Harvested corneal epithelial cell sheets before grafting, and reconstructed ocular surfaces (one week after grafting) were fixed with 10% neutral buffered formalin (Wako Chemicals). The fixed specimens were then routinely processed into 4–5-µm thick paraffin-embedded sections. Hematoxylin and eosin staining (HE) was performed by conventional methods. For immunohistochemical analyses, deparaffinized sections were treated with either anti-cytokeratin 3 (CK3) (AE5, Invitrogen, Carlsbad, CA), or anti-p63 antibody (4A4, Invitrogen) at 4 °C overnight. Secondary antibody was horseradish peroxidase (HRP) conjugated anti-mouse IgG (1:1000 dilution) (Jackson Immuno Research Laboratories, West Grove, PA). All sections were detected by 3,3'-diaminobenzidine tetrahydrochloride and counterstained with hematoxylin. Stained cells were observed under a fluorescence microscope equipped with a digital camera.

3. Results

3.1. Development of automated cell culture system (ACCS)

The ACCS developed in the present study was a whole automated cell culture platform consisting of a main culture system (MCS) (Fig. 2A) and the other systems including a refrigerator, a liquid controller, a gas controller, and a PC to control the whole system. First, cell cartridges were placed inside the MCS through the cell cartridge pass box with an air lock, and inner liquid circuits

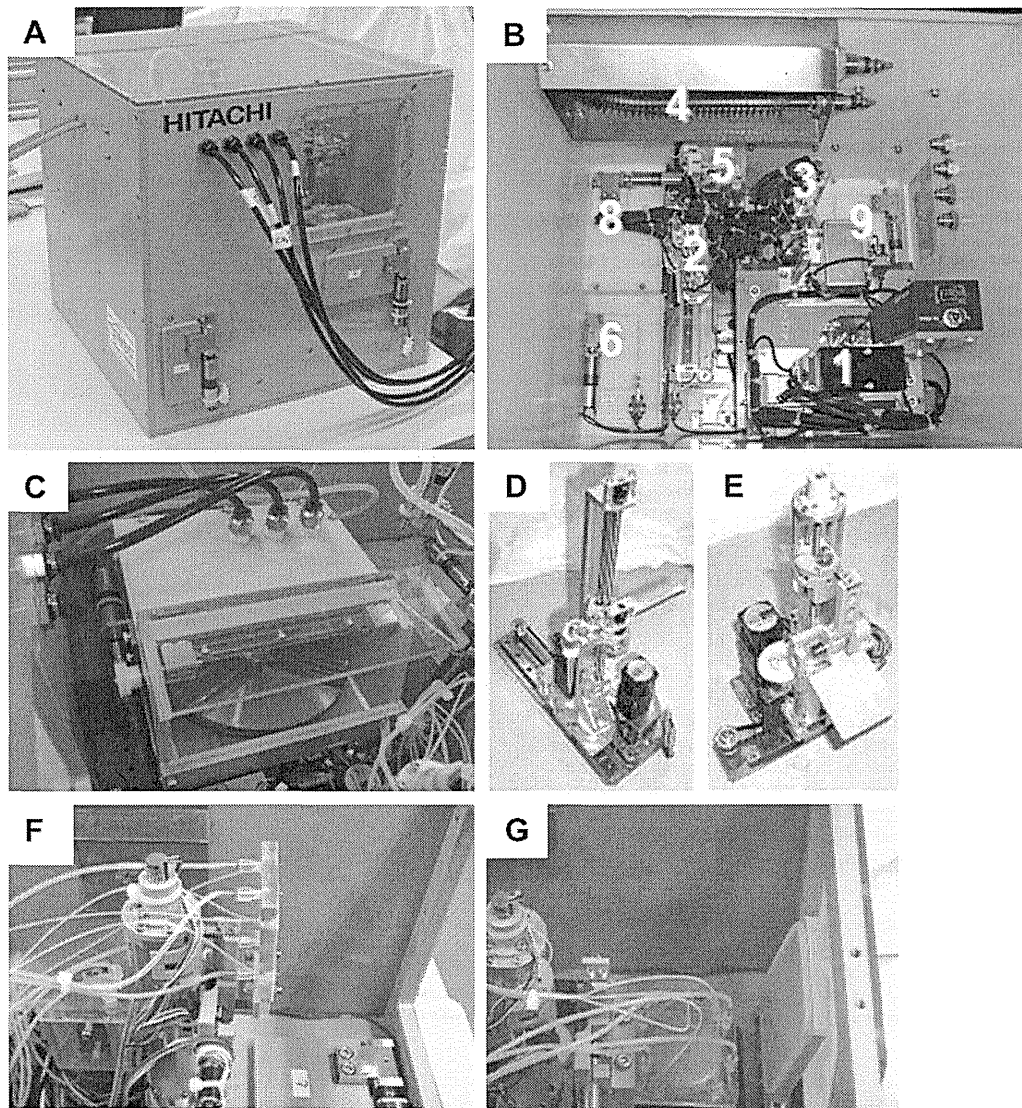


Fig. 2. The automated cell culture system. A, The front view of main culture system (MCS). B, The inside of the MCS. The main components are labeled: 1, an incubator with CCD camera; 2, a tip manipulator; 3, a handling manipulator with a connector; 4, a heater in environment controllers; 5, a liquid circuit including a tank; 6, a tip pass box with an air lock system; 7, a dust pass box with an air lock system; 8, a cell pass box with a centrifuge and an air lock system; 9, a cell cartridge pass box with an air lock system. C, The incubator. This incubator has a door and a turntable on which three cell cartridges were cultured at one time. The culture environment was kept at 37 °C, 5% CO₂, and over 95% humidity. D, The tip manipulator. E, The handling manipulator to connect with a cell cartridge and pour cells. F, The connector of the handling manipulator. G, The handling manipulator integrated with a cell cartridge in the cell cartridge pass box via its connector.

were connected with outer tubes inside a clean bench. Then, cell suspensions were injected to the MCS. Thereafter, cell culture was continued in the MCS even outside a clean bench, since the MCS was designed as airtight.

Culture medium, Dulbecco's phosphate buffer saline (PBS) to wash circuits, and waste were stored at 4 °C in the refrigerator. Aliquots of culture medium and PBS were prewarmed at 37 °C before used. The gas controller mixed air and CO₂ with valves, and supplied 5% CO₂ gas to an incubator in the MCS after filtration through a 0.22- μ m filter. The PC was connected to all the sensors and actuators via the local area network, and controlled the ACCS with the operating software running on Windows XP. This PC allowed checking out the malfunction in the system for data logging of sensor values and system errors.

The MCS was composed of nine major components (Fig. 2B–E); an incubator with CCD camera, a tip manipulator, a handling

manipulator having a connector with a cell cartridge, a liquid circuit including a tank and controllers, environment controllers, a tip pass box and a dust pass box, a cell pass box with a centrifuge, and a cell cartridge pass box. The shape of the MCS was a rectangular parallelepiped, and the size was 30 cm \times 30 cm \times 52 cm (WDH). The MCS had four air-locks (tip pass box, dust pass box, cell pass box, and cell cartridge pass box) to take culture materials (cells, cell cartridges, pipette tips, and used tips) in and out of.

The liquid circuit was semi-closed and composed of disposable tubing, two liquid tanks, connectors, and liquid bags. The two liquid bags were manually poured with culture medium and PBS inside a clean bench, respectively, then put in the refrigerator. These bags were connected with a heater to prewarm culture medium and PBS. Prewarmed liquids ran into the tanks inside the MCS to eliminate air bubble. Liquid flow was controlled with tubing pumps and

electromagnetic valves regulated by the PC. The environmental controllers kept the inner temperature at 37 °C, and supplied fresh and clean air through filters inside the MCS. Pipette tips were cleanly stored in a tip pass box with the air lock.

The whole automatic cell culture processes were divided to several tasks, and controlled by computer programs (Table 1, Supplementary video). For cell seeding, corneal epithelial cells and MMC-treated 3T3 cells were separately injected into two 2-mL tubes suspended under centrifuge arms, and cells were centrifuged. The tip manipulator automatically attached a pipette tip from a tip pass box. Cells were resuspended in culture medium by the tip manipulator at an appropriate cell concentration. Then, each cell type was transferred to each tank with the tip manipulator. Used pipette tips were dumped in the dust pass box. In the tank, the cell density was adjusted by diluting culture medium. Then, the cell cartridge handling manipulator moved to the cell cartridge pass box (Fig. 2F). A connector was equipped on the handling manipulator and connected to the circuit including the tank. The inner door of the cell cartridge pass box opened, and the connector was attached firmly to the cell cartridge (Fig. 2G). The cell cartridge integrated with the connector was rotated up 90° to the upright position, cells in each tank were separately poured into each culture room in the cell cartridge, using pumps and valves [31]. After cell injection, the front door of the CO₂ incubator was opened, and the cell cartridge was transported to a turntable in the CO₂ incubator. The cell cartridge was disconnected from the connector, and the connector moved out of the CO₂ incubator. The front door of the CO₂ incubator was closed, and cell culture started. At the same time, three cell cartridges were incubated on the turntable. To fabricate transplantable corneal epithelial cell sheets, cells were cultured for two weeks. In the incubator, temperature, humidity, and CO₂ concentration were kept 37 °C, over 95%, and 5%, respectively. Cells were monitored with a CCD camera with *x*–*z* axis movement.

Supplementary video related to this article can be found at <http://dx.doi.org/10.1016/j.biomaterials.2013.07.065>.

To exchange culture medium in cell cartridges, fresh medium from a liquid bag in the refrigerator was put into a tank through the circuit by the liquid controller with valves and pumps. Then, fresh medium was poured into each culture room in the cell cartridge integrated with the connector at the upright position. Waste liquid was collected in the waste bag in the refrigerator. Finally, the cell cartridge was transported back on a turntable in the CO₂ incubator, and disconnected from the connector.

After two-week culture, the cell cartridges were taken out of the ACCS by the following steps. The cell cartridge was integrated with the connector, and moved onto the tray in the cell cartridge pass box by the handling manipulator. After the cell cartridge pass box was separated from the rest of the ACCS by the air lock, the cell cartridge on the tray was ejected from the pass box to the outside of the ACCS.

Table 1
Automatic cell culture process.

Process	Device
Cell density adjustment	Centrifuge, tip manipulator, liquid controller
Cell cartridge transportation	Handling manipulator
Seeding cells into a cell cartridge	Handling manipulator, pump, liquid controller
Cell culture	Incubator
Medium change	Handling manipulator, pump, liquid controller
Monitoring cells	CCD camera
Environment control	Heater, gas controller

3.2. Transportation of automatically fabricated cell sheets

Often, cell processing facilities where the ACCS can be installed are far away from surgical operating rooms where tissue-engineered products fabricated with the ACCS are transplanted. In order to demonstrate the feasibility of the developed ACCS, we performed transplantation of fabricated cell sheets to an animal model after transportation by car and train. Because of temperature-responsive culture surfaces, the temperature control is a critical issue to avoid the detachment of cell sheets during transportation. Immediately after the automated cell culture, rabbit corneal epithelial cell sheets fabricated with the ACCS in Hitachi Central Research Laboratory (Saitama, Japan) were transported to the Medical School of Osaka University (Osaka, Japan) to transplant them. The distance of the two sites was 581 km. A portable homothermal container (30 cm in diameter of the top, 27.5 cm in height) that allowed a constant inner temperature of 36 °C during transportation was used [29]. The wall of the container had vacuum heat insulation to minimize heat loss. At the core of the homothermal container, a small inner chamber was installed, and the top and bottom of the inner chamber were directly contacted with copper plates to make heat distribution uniform. Within the inner chamber was filled with a heat shortage material, *n*-eicosane, in plastic bags. Cell cartridges were placed at the center of the inner chamber during transportation and surrounded by the heat storage material. This container didn't need batteries or energy supply to keep inner temperature at 36 °C. The extra space inside the portable container was occupied by an adiabatator to reduce heat loss. With the portable container, cell sheets fabricated on temperature-responsive culture surfaces were transported for 6 h and 20 min by car and train. The portable container kept the inner temperature at 36.1 ± 0.1 °C, although the outer temperature was significantly changed (Fig. 3).

Primary rabbit limbal epithelial cells were seeded at the density of 2.0×10^4 cells/cm² into the cell cartridges inside the ACCS (Fig. 4A), and cultured for two weeks. The rate of the viable cells was 93.6%. The rate of putative progenitor cells was 8.9%. During two weeks, the ACCS automatically changed culture medium totally ten times. Cultured cells grew to confluency, and were multi-layered (Fig. 4B). Even after transportation in the container, all the cells in cell cartridges still intactly adhered on the temperature-responsive culture surfaces and no cell morphological changes were observed (Fig. 4C).

After the transportation, cell cartridges were transferred to CO₂ incubator at 20 °C and 5% CO₂ in an operation room for the transplantation. Within 30 min, all the cells were detached from the

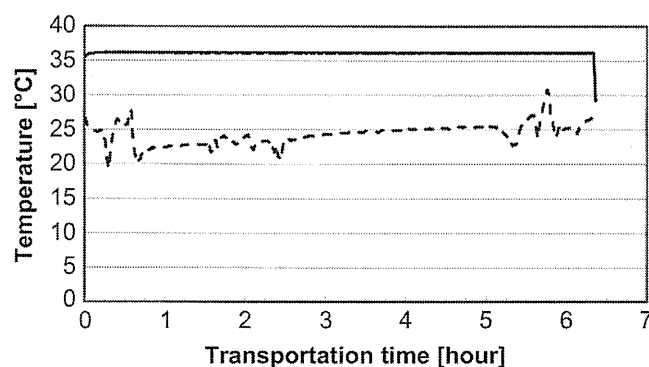


Fig. 3. Temperature change of the inside and outside of the homothermal container. Cell cartridges were transported by train and car for 6 h and 20 min. Each line shows the temperature inside (solid line) or outside the container (dashed line).

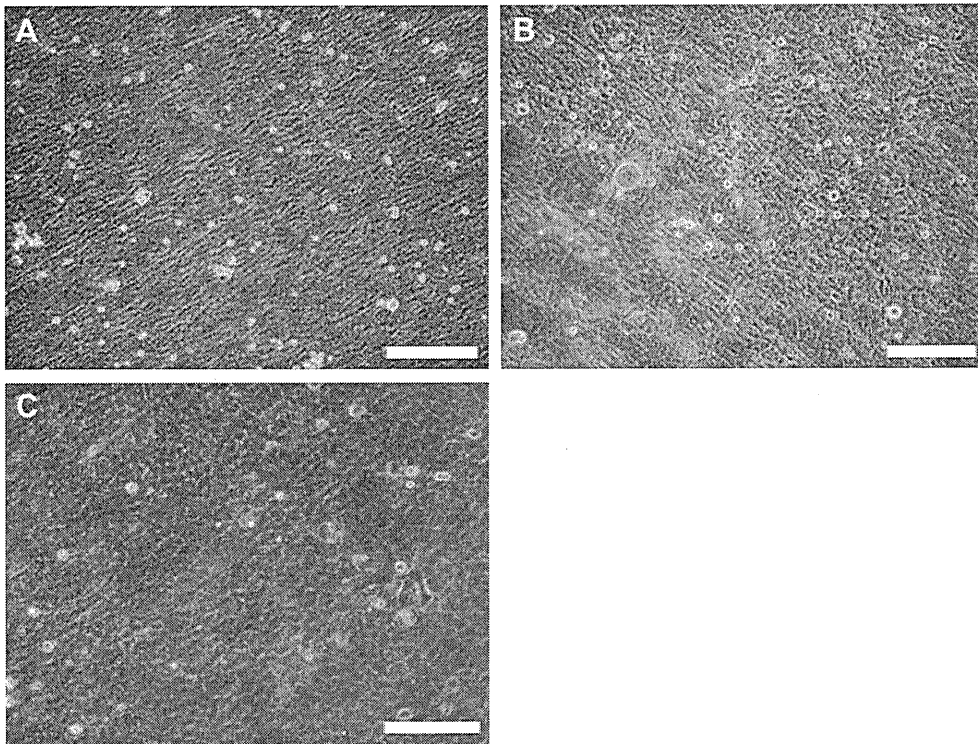


Fig. 4. Phase-contrast microscopic images of cultured rabbit corneal epithelial cells. A, Seeded cells into the cell cartridges using the ACCS. B, Cells cultured for two weeks in the ACCS. C, Cells transported for 6 h and 20 min in the transport container. Bars = 250 μm .

temperature-responsive culture surface as a single continuous cell sheet [8].

Harvested cell sheets were examined by histological evaluation with HE staining and immunofluorescence. The cell sheets comprised of three to five stratified and well-differentiated cell layers (Fig. 5A). p63, a putative epithelial stem/putative marker [32] was detected in the nuclei of the basal cell layers (Fig. 5C). CK3 served as a negative marker for epithelial stem cells [33] was absent from the basal layers (Fig. 5E). These results suggest that harvested cell sheets contain putative stem/progenitor cells in the basal cells.

3.3. Transplantation

Automatically cultured, and transported cell sheets were successfully transplanted onto ocular surfaces in a rabbit corneal stem cell deficiency model [34]. Transplanted corneal epithelial cell sheets readily resisted displacement under tension with forceps, implying stable adhesion to the corneal stroma. Damaged ocular surfaces in the model became clouded (Fig. 6A) and failed to repel fluorescein penetration into the stroma before cell sheet transplant (Fig. 6C). However, corneal surfaces became clear and smooth (Fig. 6B) and were completely protected from fluorescein penetration by grafted cell sheets immediately after a week from transplant (Fig. 6D). Ocular surfaces were completely reconstructed with faint or no observable defects. After observation, rabbits were sacrificed under an anesthetic, and the eyes were examined by histological evaluation with HE staining and immunofluorescence. The transplanted cell sheets existed on stroma surface and gaps between regenerated epithelium and stroma, underlying stromal vascularization inflammatory cells, and goblet cells were not observed in corneas receiving cell sheet-transplants (Fig. 5B). p63 was detected in the nuclei of the basal cell layers (Fig. 5D). CK3 was absent from the basal layers, but expressed in the mature corneal

epithelium (Fig. 5F). These results imply that reconstructed ocular surfaces had basal layers containing putative stem/progenitor cells, and multi-layered epithelial structure resembling native corneal epithelium morphologically.

4. Discussion

Conventionally, the culture operation to fabricate transplantable epithelial cell sheets was manually performed using open culture vessels such as 6-well plates with culture inserts [9]. Nowadays, in order to improve the efficiency and safety of cell culture process, several ACCSs have been developed. ACCS which has a robotic arm is already commercially available [22–25]. These ACCSs are designed to use conventional open culture vessels, and mimic the manual process as closely as possible to avoid process modifications based on assumptions about the sources of process output variation. Continuous operation of the robotic arm achieves scale-up of cell culture and fabrication of tissue-engineered products [23]. However, it is quite difficult for ACCSs which has a single robotic arm to handle culture inserts in 6-well plates that are commonly used to fabricate epithelial cell sheets. When an additional robotic arm is installed, the size of ACCSs should be bigger, and the ACCSs need larger air-conditioning units with HEPA filter. In addition, the use of conventional open vessels such as culture inserts in 6-well plates would not be appropriate for transportation in clinical settings, and require a special container to prevent contamination.

An ACCS using a closed culture vessel connected to a closed circuit was also reported [26]. This system was designed to expand bone marrow-derived mesenchymal stem cells. Since this system uses its original culture vessels, it doesn't accept epithelial cell culture using feeder layer separated by microporous membrane. An FDA-approved, tissue-engineered product, Dermagraft is fabricated

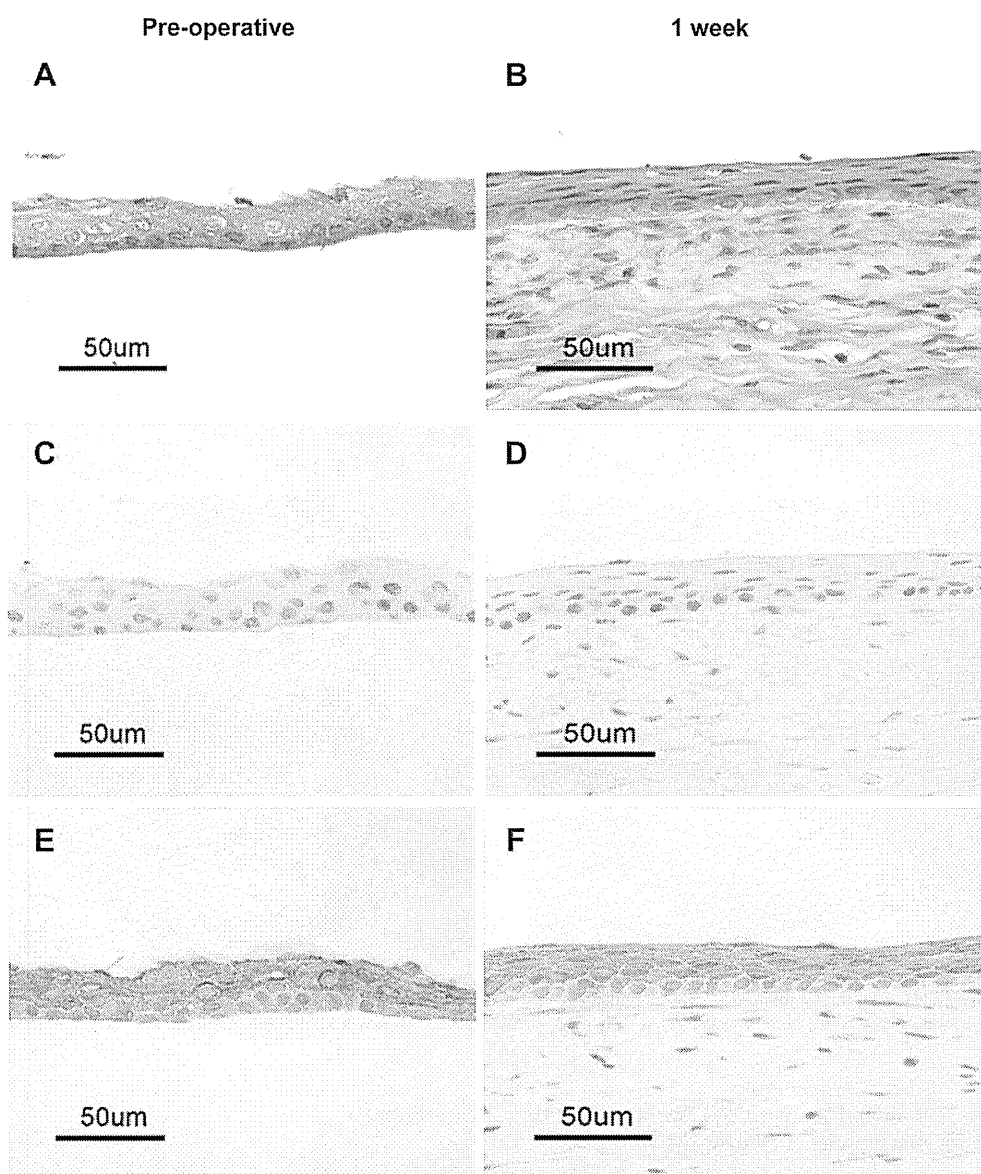


Fig. 5. Histology. Left panels show transplantable epithelial cell sheets fabricated with the ACCS. Right panels show rabbit cornea one week after the transplantation. A, B, HE staining. C, D, Immunohistochemistry with anti-p63 antibody. E, F, Immunohistochemistry with anti-CK3 antibody. Bars = 50 μ m.

with its customized bioreactor using closed culture vessels connected to a closed circuit [35]. After culture of foreskin dermal fibroblasts on biodegradable scaffolds in the vessels, each vessel containing an individual piece of Dermagraft was sealed, and then cut out of the bioreactor. This individual piece of a closed culture vessel is safe to transport, and shipped to the customer. Since Dermagraft is an allogeneic product and mass production in each lot is performed, the design of the closed culture vessel is appropriate. Since transplantable epithelial cell sheets to treat limbal stem cell deficiency are fabricated with patients' own cells in an autologous manner, small production for each patient is performed.

In the present study, a prototype of the ACCS based on a concept using double-layered closed cell culture vessels [28] and miniaturization of MCS was developed. The cell cartridge was connected to a closed circuit only in cell seeding and medium change, then disconnected and cultured [31]. The closed culture vessels were tiny and easy to transport. Actually, we successfully performed automatic fabrication of transplantable corneal epithelial cell

sheets with the ACCS, transported them with a portable homeothermal container [29], and finally transplanted to a rabbit corneal stem cell deficiency model. The ocular surfaces were reconstructed one week after transplantation as previously shown with manually fabricated cell sheets [8].

Since the size of MCS in the present ACCS was small, a number of MCSs culturing cells of different patients can be connected with a single refrigerator and a single controller. Therefore, autologous products for different patients can be fabricated at one time in a single clean room of CPF. Since the employment and training of operators can be reduced to the minimum by using ACCSs, the production cost can be saved, and the safe and stable mass production of tissue-engineered products can be achieved.

In the future, manual productions of tissue-engineered products in expensive and large facilities would be completely replaced with automated factories full of ACCSs as observed with automobile and semiconductor industries. New technologies such as ACCSs and

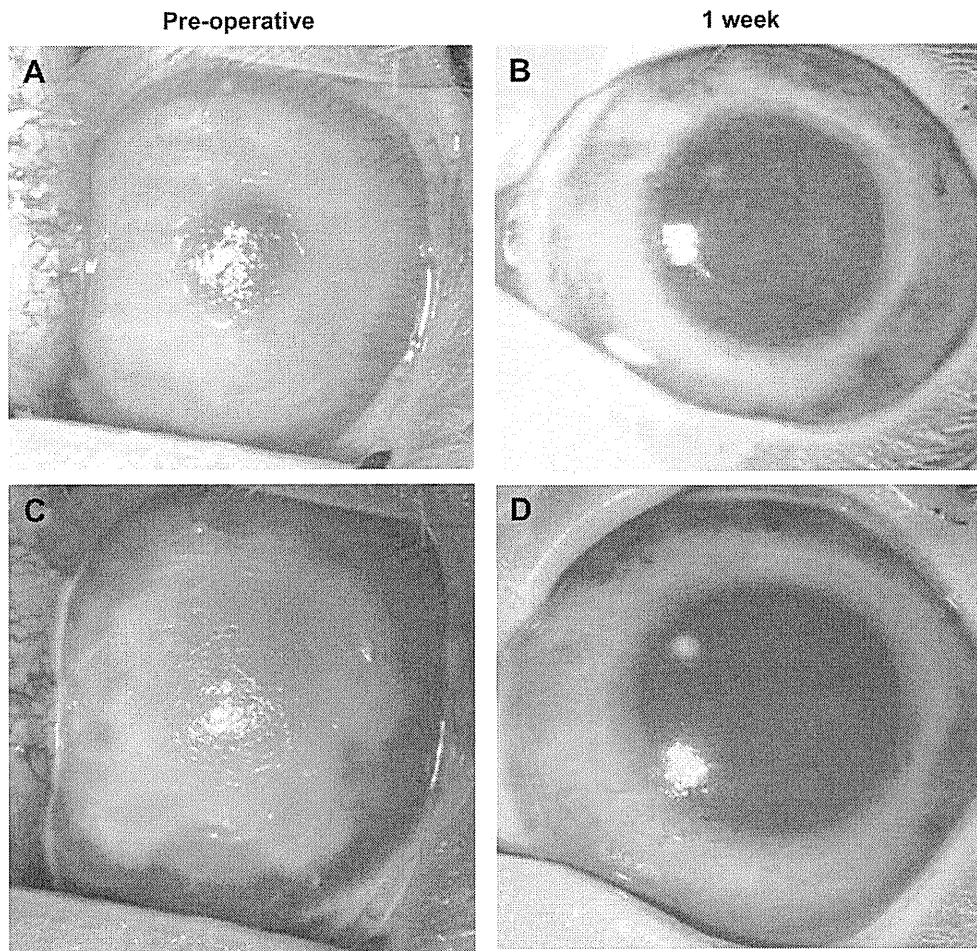


Fig. 6. Reconstruction of ocular surfaces by transplantation of corneal epithelial cell sheets fabricated with the ACCS. Left panels show preoperative ocular surfaces. Right panels show reconstructed ocular surfaces one week after the transplantation. A, B, Macroscopic view. C, D, Fluorescent images of ocular surfaces after fluorescein staining.

transportation devices [29] should increase the opportunities of regenerative medicine for many patients all over the world.

5. Conclusions

Here, we developed a prototype of a small automated cell culture system with closed culture vessels called cell cartridge. Transplantable corneal epithelial cell sheets were automatically fabricated with the system, transported, and successfully transplanted rabbit corneal stroma. Such the devices would promote regenerative medicine in the future clinical settings.

Acknowledgments

The authors are grateful for the support of Dr. T. Nozaki, Dr. S. Takeda (Hitachi), Mr. T. Inuma (Hitachi Transport System), Mr. H. Sugiyama, Dr. M. Mizutani, Mr. H. Sakai (CellSeed) and Dr. T. Soma (Osaka University). This work was supported in part by the Basic Technologies Research Promotion Project “Development of Nano-bio Interface Technologies for Tissue Regeneration Implant” from New Energy and Industrial Technology Development Organization (NEDO), Japan, and the Creation of Innovation Centers for Advanced Interdisciplinary Research Areas Program in the Project for Developing Innovation Systems “Cell Sheet Tissue Engineering Center (CSTEC)” from the Ministry of Education, Culture, Sports, Science and Technology (MEXT), Japan.

References

- [1] Kwon OH, Kikuchi A, Yamato M, Sakurai Y, Okano T. Rapid cell sheet detachment from poly(N-iso-propylacrylamide)-grafted porous cell culture membranes. *J Biomed Mater Res* 2000;50:82–9.
- [2] Kushida A, Yamato M, Konno C, Kikuchi A, Okano T. Decrease in culture temperature releases monolayer endothelial cell sheets together with deposited fibronectin matrix from temperature-responsive culture surfaces. *J Biomed Mater Res* 1999;45:355–62.
- [3] Kushida A, Yamato M, Kikuchi A, Okano T. Two-dimensional manipulation of differentiated Madin-Darby canine kidney (MDCK) cell sheets: the noninvasive harvest from temperature-responsive culture dishes and transfer to other surfaces. *J Biomed Mater Res* 2001;54:37–46.
- [4] Kushida A, Yamato M, Isoi Y, Kikuchi A, Okano T. A noninvasive transfer system for polarized renal tubule epithelial cell sheets using temperature-responsive culture dishes. *Eur Cell Mater* 2005;10:23–30.
- [5] Shimizu T, Yamato M, Isoi Y, Akutsu T, Setomaru T, Abe K, et al. Fabrication of pulsatile cardiac tissue grafts using a novel 3-dimensional cell sheet manipulation technique and temperature-responsive cell culture surfaces. *Circ Res* 2002;90:e40.
- [6] Yamada N, Okano T, Sakai H, Karikusa F, Sawasaki Y, Sakurai Y. Thermo-responsive polymeric surfaces; control of attachment and detachment of cultured cells. *Makromol Chem Rapid Commun* 1990;11:571–6.
- [7] Yamato M, Utsumi M, Kushida A, Konno C, Kikuchi A, Okano T. Thermo-responsive culture dishes allow the intact harvest of multilayered keratinocyte sheets without disperse by reducing temperature. *Tissue Eng* 2001;7:473–80.
- [8] Nishida K, Yamato M, Hayashida Y, Watanabe K, Maeda N, Watanabe H, et al. Functional bioengineered corneal epithelial sheet grafts from corneal stem cells expanded ex vivo on a temperature-responsive cell culture surface. *Transplantation* 2004;77:379–85.
- [9] Nishida K, Yamato M, Hayashida Y, Watanabe K, Yamamoto K, Adachi E, et al. Corneal reconstruction with tissue-engineered cell sheets composed of autologous oral mucosal epithelium. *N Engl J Med* 2004;351:1187–96.

- [10] Ohki T, Yamato M, Ota M, Takagi R, Murakami D, Kondo M, et al. Prevention of esophageal stricture after endoscopic submucosal dissection using tissue-engineered cell sheets. *Gastroenterology* 2012;143:582–8.
- [11] Takagi R, Murakami D, Kondo M, Ohki T, Sasaki R, Mizutani M, et al. Fabrication of human oral mucosal epithelial cell sheets for treatment of esophageal ulceration by endoscopic submucosal dissection. *Gastrointest Endosc* 2010;72:1253–9.
- [12] Sawa Y, Miyagawa S, Sakaguchi T, Fujita T, Matsuyama A, Saito A, et al. Tissue engineered myoblast sheets improved cardiac function sufficiently to discontinue LVAS in a patient with DCM: report of a case. *Surg Today* 2012;42:181–4.
- [13] Iwata T, Yamato M, Tsuchioka H, Takagi R, Mukobata S, Washio K, et al. Periodontal regeneration with multi-layered periodontal ligament-derived cell sheets in a canine model. *Biomaterials* 2009;30:2716–23.
- [14] Ebihara G, Sato M, Yamato M, Mitani G, Kutsuna T, Nagai T, et al. Cartilage repair in transplanted scaffold-free chondrocyte sheets using a minipig model. *Biomaterials* 2012;33:3846–51.
- [15] Takagi R, Yamato M, Murakami D, Kondo M, Ohki T, Sasaki R, et al. Fabrication and validation of autologous human oral mucosal epithelial cell sheets to prevent stenosis after esophageal endoscopic submucosal dissection. *Pathobiology* 2011;78:311–9.
- [16] Archer R, Williams DJ. Why tissue engineering needs process engineering. *Nat Biotechnol* 2005;23:1353–5.
- [17] Dutton RL, Fox JS. Robotic processing in barrier-isolator environments: a life cycle cost approach. *Pharm Eng* 2006;26:1–8.
- [18] Thomas RJ, Hourd PC, Williams DJ. Application of process quality engineering techniques to improve the understanding of the in vitro processing of stem cells for therapeutic use. *J Biotechnol* 2008;136:148–55.
- [19] Liu Y, Hourd P, Chandra A, Williams DJ. Human cell culture process capability: a comparison of manual and automated production. *J Tissue Eng Regen Med* 2010;4:45–54.
- [20] Mason C, Hoare M. Regenerative medicine bioprocessing: building a conceptual framework based on early studies. *Tissue Eng* 2007;13:301–11.
- [21] Kino-oka M, Taya M. Recent developments in processing systems for cell and tissue cultures toward therapeutic application. *J Biosci Bioeng* 2009;108:267–76.
- [22] Chang A, Stephan JP. Is the dream becoming reality. *Eur Pharm Rev* 2006;6:46–51.
- [23] Thomas RJ, Chandra A, Hourd PC, Williams DJ. Cell culture automation and quality engineering: a necessary partnership to develop optimized manufacturing processes for cell-based therapies. *J Lab Autom* 2008;13:152–8.
- [24] Thomas RJ, Anderson D, Chandra A, Smith NM, Young LE, Williams D, et al. Automated, scalable culture of human embryonic stem cells in feeder-free conditions. *Biotechnol Bioeng* 2009;102:1636–44.
- [25] Knoll A, Scherer T, Poggendorf I, Lütkemeyer D, Lehmann J. Flexible automation of cell culture and tissue engineering tasks. *Biotechnol Prog* 2004;20:1825–35.
- [26] Kato R, Iejima D, Agata H, Asahina I, Okada K, Ueda M, et al. A compact, automated cell culture system for clinical scale cell expansion from primary tissues. *Tissue Eng Part C Methods* 2010;16:947–56.
- [27] Takagi R, Yamato M, Murakami D, Kondo M, Yang J, Ohki T, et al. Preparation of keratinocyte culture medium for the clinical applications of regenerative medicine. *J Tissue Eng Regen Med* 2011;5:e63–73.
- [28] Nakajima R, Kobayashi T, Moriya N, Mizutani M, Kan K, Nozaki T, et al. A novel closed cell culture device for fabrication of corneal epithelial cell sheets. *J Tissue Eng Regen Med* 2012. <http://dx.doi.org/10.1002/term.1639> [Epub ahead of print].
- [29] Nozaki T, Yamato M, Inuma T, Nishida K, Okano T. Transportation of transplantable cell sheets fabricated with temperature-responsive culture surface for regenerative medicine. *J Tissue Eng Regen Med* 2008;2:190–5.
- [30] Tsai RJ, Li LM, Chen JK. Reconstruction of damaged corneas by transplantation of autologous limbal epithelial cells. *N Engl J Med* 2000;343:86–93.
- [31] Kobayashi T, Kan K, Koide A, Sakai H. Culturing apparatus. US Patent No. 0115893, 2006.
- [32] Pellegrini G, Dellambra E, Golisano O, Martinelli E, Fantozzi I, Bondanza S, et al. p63 identifies keratinocyte stem cells. *Proc Natl Acad Sci U S A* 2001;98:3156–61.
- [33] Harkin DG, Barnard Z, Gillies P, Ainscough SL, Apel AJ. Analysis of p63 and cytokeratin expression in a cultivated limbal autograft used in the treatment of limbal stem cell deficiency. *Br J Ophthalmol* 2004;88:1154–8.
- [34] Ang LP, Tanioka H, Kawasaki S, Ang LP, Yamasaki K, Do TP, et al. Cultivated human conjunctival epithelial transplantation for total limbal stem cell deficiency. *Invest Ophthalmol Vis Sci* 2010;51:758–64.
- [35] Mansbridge J. Commercial considerations in tissue engineering. *J Anat* 2006;209:527–32.